Nur77 Prevents Excessive Osteoclastogenesis by Inducing Ubiquitin Ligase Cbl-b to Mediate NFATc1 Self-Limitation

Xiaoxiao Li[1], Wei Wei[1], HoangDinh Huynh[1] and Yihong Wan[1]

[1]Department of Pharmacology, The University of Texas Southwestern Medical Center, Dallas, Texas 75390, USA

Approved by Supervisory Committee

Yihong Wan, PhD

Carole Mendelson, PhD

Andrew Zinn, MD/PhD

Steve Kliewer, PhD

To Mom, Dad, M. B. and M. E.

Nur77 Prevents Excessive Osteoclastogenesis by Inducing Ubiquitin Ligase Cbl-b to Mediate NFATc1 Self-Limitation

Xiaoxiao Li

DISSERTATION /THESIS

Presented to the Faculty of the Graduate School of Biomedical Sciences

The University of Texas Southwestern Medical Center at Dallas

In Partial Fulfillment of the Requirements

For the Degree of

DOCTOR OF PHILOSOPHY .

The University of Texas Southwestern Medical Center

Dallas, Texas

May, 2017

Nur77 Prevents Excessive Osteoclastogenesis by Inducing Ubiquitin Ligase Cbl-b to Mediate NFATc1 Self-Limitation

XIAOXIAO LI, Ph.D

The University of Texas Southwestern Medical Center at Dallas, 2015

YIHONG WAN, Ph.D.

Osteoclasts are bone-resorbing cells essential for skeletal remodeling. However, over-active osteoclasts can cause bone degenerative disorders. Therefore, the level of NFATc1, the master transcription factor of osteoclast, must be tightly controlled. Although the activation and amplification of NFATc1 have been extensively studied, how NFATc1 signaling is eventually resolved is unclear. Here, we uncover a novel and critical role of the orphan nuclear receptor Nur77 in mediating an NFATc1 self-limiting regulatory loop to prevent excessive osteoclastogenesis. Nur77 deletion leads to low bone mass owing to augmented osteoclast differentiation and bone resorption. Mechanistically, NFATc1 induces Nur77 expression at late stage of osteoclast differentiation; in turn, Nur77 transcriptionally up-regulates E3 ubiquitin ligase Cbl-b, which triggers NFATc1 protein degradation. These findings not only identify Nur77 as a key player in osteoprotection and a new therapeutic target for bone diseases, but also elucidate a previously unrecognized NFATc1→Nur77→Cblb—•NFATc1 feedback mechanism that confers NFATc1 signaling autoresolution.

TABLE OF CONTENTS

LIST OF FIGURES

Introduction

Osteoporosis is a debilitating disease that affects more than 75 million people in the United States, Europe and Japan.(Kanis, 1994) It is characterized by low bone mass, or bone mineral density, which can lead to increased risk of fracture. Although osteoporosis is more prevalent in white postmenopausal females, it occurs in all populations and at all ages. It is estimated that the lifetime risks of osteoporotic fracture for women and men are at 44% and 25%, respectively. (Nguyen et al., 2007) Bone fractures result in skeletal deformity, pain, increased mortality, and severe economic burden for society. (2001)

Bone health is intimately related to the balance of bone-forming cells osteoblasts, and bone-resorbing osteoclast cells. Imbalance of the two, most commonly over-activation of osteoclasts, can lead to decreased bone density and fracture. In addition to osteoporosis, osteoclast over-activation has also been implicated in rheumatoid arthritis (Tanaka, 2013), and breast, prostate, kidney and lung cancer metastasis to the bone (Roodman, 2004), and hypercalcemia of malignancy(Bruzzaniti and Baron, 2006)

Osteoclasts are multi-nucleated giant cells derived from myeloid progenitor cells upon RANKL (Receptor Activator of Nuclear Factor Kappa-B Ligand) signaling. A member of the tumor necrosis factor receptor (TNFR), RANK lacks intrinsic enzymatic activity and rely on adaptor proteins such as tumor necrosis factor receptor-associated factor 6 (TRAF6) and Grb-2-associated binder-2 (Gab2) to

transduce signals from RANKL. (Kuroda and Matsuo, 2012) These adaptor proteins rapidly induce diverse signaling pathways such as Akt kinase, JUNK, p38, leading to the transcription of NF-kB and AP-1. (Kuroda and Matsuo, 2012) NF-kB and AP1 are composed of two molecules among p65, RelB, p50 and p52 (for NF-kB) and JunB, c-Fos and c-Jun (for AP1). About 24 hrs after RANKL stimulation, oscillating intracellular calcium levels activates calcineurin, which dephosphorylates NFATc1 and induces its nuclear translocation. NFATc1 in turn turns on genes that mediate osteoclast progenitor cell-fusion, maturation and bone resorption activity. (Schett et al., 2005) A schematic representation of the RANKL signaling pathway in osteoclast is represented below (**Figure 1.0)**. (Boyce and Xing, 2007a)

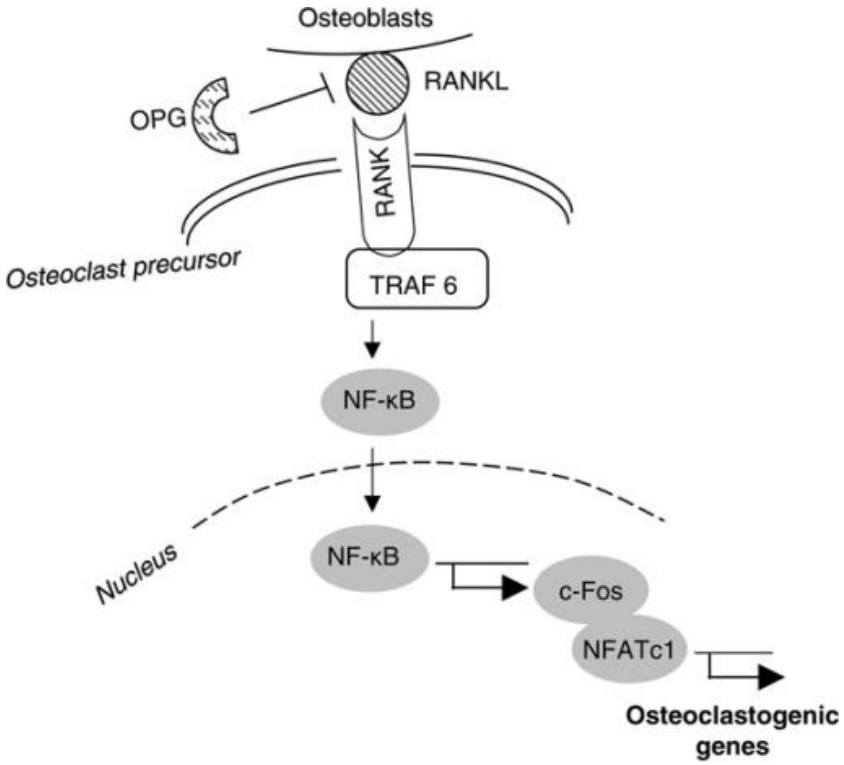

(Figure 1.0). RANKL signaling in osteoclast

NFATc1 is a key transcriptional switch that activates osteoclastogenesis. Ectopic NFATc1 expression alone in osteoclast precursors is sufficient to produce mature osteoclasts, whereas NFATc1 deletion blocks the ability of the precursors to differentiate into osteoclasts (Takayanagi et al., 2002). NFATc1 binds to its response elements containing a consensus sequence of GGAAA, and its target genes in osteoclasts include cathepsin K, CLC-7 chloride channel, vacuolar proton pump subunit Atp6v0d2, etc. (Kuroda and Matsuo, 2012). NFATc1 has been shown to auto-amplify during osteoclast differentiation, and this auto-amplification process has been suggested to be important for osteoclast lineage commitment (Asagiri et al., 2005). However, so far very few studies have dealt with whether and how NFATc1 signaling is attenuated upon its initial activation. As a result, despite the crucial functions of NFATc1 in osteoclastogenesis, the mechanisms for how NFATc1 signaling is resolved to prevent excessive osteoclast differentiation are still incompletely understood.

Nur77 (or NR4A1), also known as nerve growth factor IB (NGFIB), TR3 or NAK-1, is an orphan nuclear receptor in the NR4A family, which also includes Nurr1 (NR4A2) and Nor1 (NR4A3). Nur77 is composed of an amino-terminal trans-activation domain, a central DNA-binding domain and a carboxy-terminal ligand-binding domain (LBD). Unlike other members of the nuclear receptor family, however, Nur77 possess an atypical LBD with hydrophilic cleft and distinct

topology.(Wansa et al., 2002) Furthermore, Nur77 has an constitutively active transcriptional activity independent of ligand binding, since Nur77 mutant with truncated LBD has the same activity as wild type protein. (Paulsen et al., 1992) As a result, Nur77 activity is mostly regulated at the transcriptional level and post-transcription modification such as phosporylation.(Paulsen et al., 1992) Interestingly, expression of Nur77 can be rapidly induced by a variety of stimuli such as fatty acids, stress, prostaglandins, growth factors, calcium, inflammatory cytokines, peptide hormones, phorbol esters, neurotransmitters, membrane deporlarization, magnetic fields and mechanical agitation. (Maxwell and Muscat, 2006)

Nur77 can bind to NurRE or NBRE as monomer, homodimer or heterodimer (Philips et al., 1997), and DR5 as a heterdimer with RXR (Perlmann and Jansson, 1995). Nur77 has been implicated in a variety of physiological processes, including thymocyte negative selection, hypothalamic-pituitary adrenal axis, chronic inflammation, and vascular smooth muscle cell proliferation (Hsu et al., 2004). In addition, recent studies have demonstrated Nur77's role in myeloid progenitors, which are osteoclast precursor cells. Loss of Nur77 and Nor1, a closely related nuclear receptor in the same NR4A family in mice can lead to lethal acute myeloid leukemia (AML), with abnormal expansion of myeloid progenitors, decreased expression of the AP-1 transcription factors JunB and c-Jun and defective extrinsic apoptotic (Fas-L and TRAIL) signaling.(Mullican et al., 2007) Nonetheless, it is unknown whether Nur77 can directly regulate skeletal homeostasis or bone cell differentiation.

Casitas B-lineage lymphoma proto-oncogene-b (Cbl-b) is an important E3 ligase that modulates of immune activation and dampens immune responses. (Lutz-Nicoladoni et al., 2015) The mammalian genome encodes three Cbl proteins: c-Cbl, Cbl-b and Cbl-c. The genes that code these proteins are highly conserved and can be found from nematodes to mammals (Nau and Lipkowitz, 2003). All three mammalian Cbl proteins are RING-type E3 ligases containing a N-terminal tyrosine kinase binding (TKB) domain, a Src homology (SH2) domain, and the RING domain. Cbl-b function has been implicated in negative regulation of T cell activation (Paolino and Penninger, 2010), natural killers cells (NK) (Paolino et al., 2014), dendritic cells (Chiou et al., 2011), B cells (Qiao et al., 2007) and myeloid cells (Hirasaka et al., 2007). In the skeletal system, Cbl-b has been shown to increase osteoclast activity and bone resorption, without affecting osteoblast activity. (Nakajima et al., 2009)

Current treatment options for osteoporosis are very limited, with most of them focusing on inhibiting osteoclast activity. Denozumab, approved by FDA in 2010, is a human monoclonal antibody that inhibits RANKL, thereby limiting osteoclast differentiation and activity. The most commonly prescribed drugs are bisphosphonates such as alendronate, which function by inhibiting osteoclast activity, although the exact mechanisms are not well understood and somewhat contradictory. (Weinstein et al., 2009) Furthermore, bisphosphonates have a variety of undesirable side effects. Oral intake of bisphosphonates causes esophageal burn and erosion. When administered intravenously to treat cancer, they can cause osteonecrosis of the

jaw (ONJ). Furthermore, bisphosphonates have recently been shown to increase the risk of fracture after prolonged use (Whitaker et al., 2012). Therefore, it is necessary to identify and study new genes and pathways that regulate osteoclastogenesis to potentially expand our therapeutic options.

In this study, I uncovered a novel and important role of Nur77 in NFATc1 protein degradation during osteoclastogenesis and bone resorption, thus revealing a previously unrecognized mechanism that is essential for the resolution of NFATc1 signaling in which NFATc1 exerts self-limitation via an NFATc1→Nur77→Cblb—•NFATc1 negative feedback loop. In addition, I studied Nur77's role in bone related diseases such as fracture healing, cancer metastasis to the bone, rheumatoid arthritis and explored several options to activate Nur77 pathway to treat these diseases. Finally I described the novel phenomena of how loss of Nur77 in foster parents can alter pup's bone phenotype.

Results

Nur77 Deletion Enhances Osteoclast Differentiation

To examine the expression pattern of Nur77 during osteoclast differentiation, I treated bone marrow-derived osteoclast precursor cells with RANKL for 4 days (**Figure 1A**). A time course analysis showed that Nur77 expression started to rise on day 2 during osteoclastogenesis (**Figure 1B**). The other two members of the NR4A family, Nurr1 and NOR1, were either not expressed or expressed at much lower levels (**Figure 1B**).

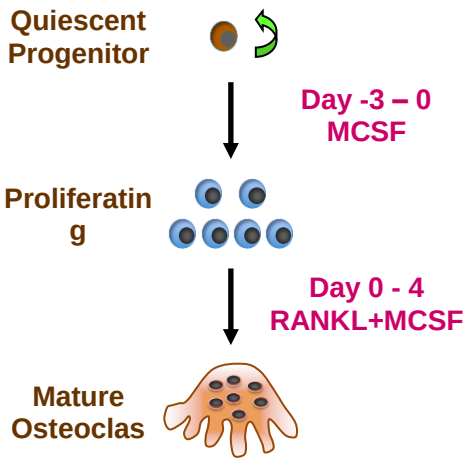

(Figure 1 A) A schematic diagram of *ex vivo* bone marrow osteoclast differentiation.

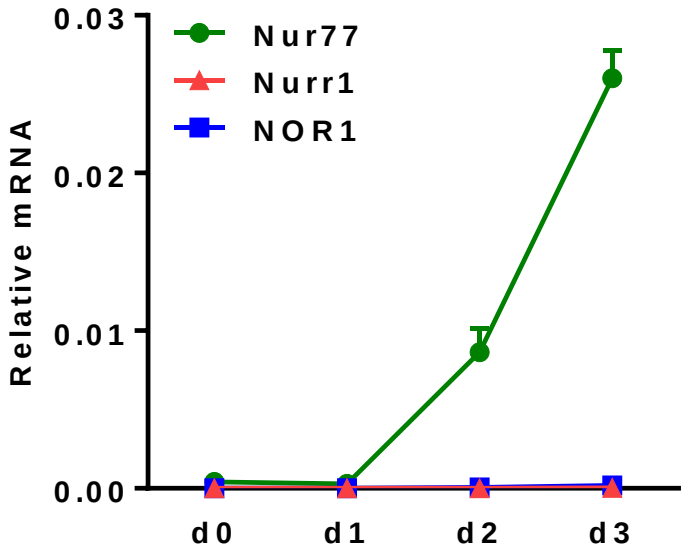

(Figure 1B) Nur77, Nurr1, and Nor1 expression during a time course of RANKL-induced osteoclast differentiation (n=3).

To determine if there is any potential regulatory role of Nur77 in osteoclastogenesis, I compared osteoclast differentiation cultures from bone marrow hematopoietic progenitors of Nur77 knockout (KO, *Nur77-/-*) mice and WT littermate controls. The results revealed an enhanced osteoclast differentiation in Nur77-KO cultures shown by the higher expression of osteoclast differentiation markers such as tartrate-resistant acid phosphatase (TRAP), cathepsin K (CTSK),

calcitonin receptor (CALCR), carbonic anhydrase 2 (CAR2), as well as the master osteoclastogenic transcription factor NFATc1 (**Figure 1C**). Consistent with these results, I have also observed more and larger mature osteoclasts in the differentiation cultures by TRAP staining (**Figure 1D**).

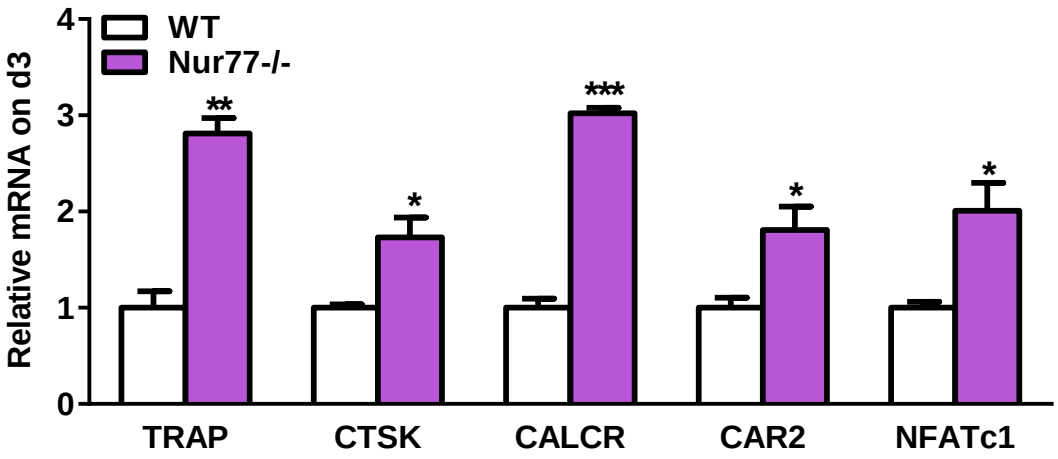

(Figure 1C) Expression of osteoclast differentiation markers on day 3 (n=4).

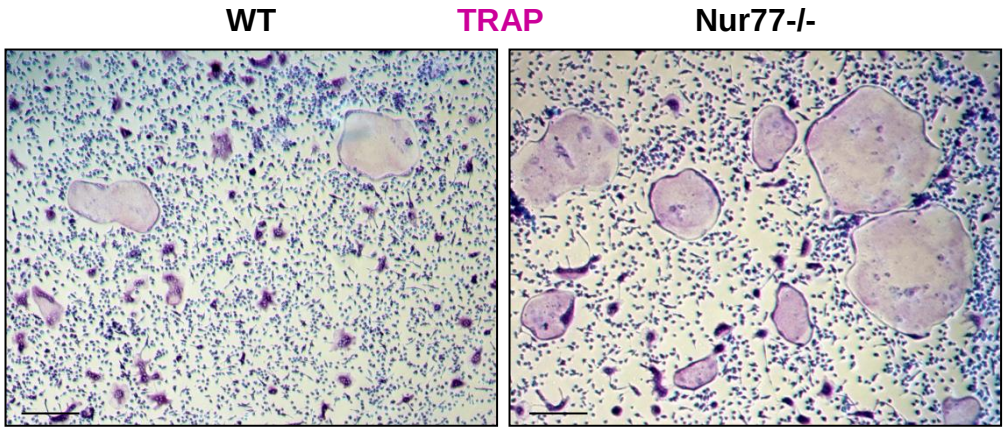

(Figure 1D) Representative images of the TRAP-stained osteoclast differentiation cultures. Mature osteoclasts were identified as multinucleated $TRAP^{+}$ (purple) cells on day 9. Scale bar, 25μm.

In contrast, osteoblast differentiation from Nur77-KO bone marrow mesenchymal progenitors was unaltered, shown by the similar induction of osteoblast markers such as collagen, type I, alpha 1 (Col1a1) and osteocalcin (**Figure 1E**). These results suggest that Nur77 may specifically suppress osteoclastogenesis during bone remodeling.

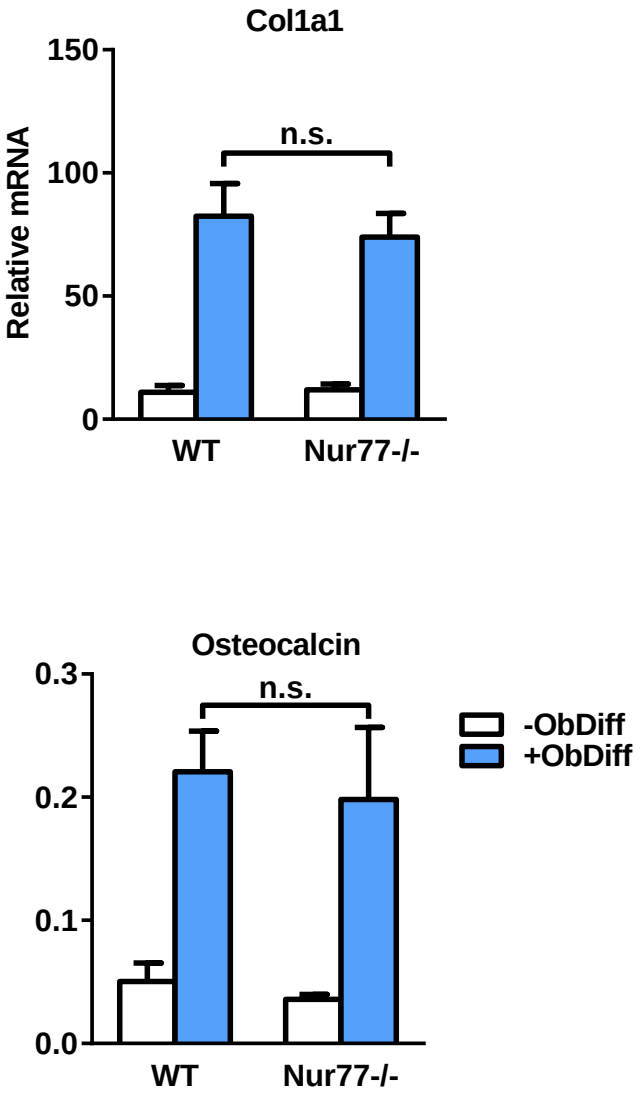

(Figure 1E) Osteoblast differentiation was unaltered in Nur77-KO cultures, measured by the expression of osteoblast markers (n=4).

Nur77 Deletion Leads to Bone Loss Due to Excessive Bone Resorption

To determine whether Nur77 is a physiologically significant regulator of bone, I next examined the *in vivo* skeletal phenotype of Nur77-KO mice. MicroCT analysis revealed that Nur77-KO mice had a low-bone-mass compared to WT littermate controls (**Figure 1F**), illustrated by a 36% lower bone volume/tissue volume ratio (BV/TV) (**Figure 1G**), 19% less bone surface (BS) (**Figure 1H**), 8% greater bone volume/bone surface ratio (BV/BS) (**Figure 1I**), 14% less trabecular number (Tb.N) (**Figure 1J**), 8% less trabecular thickness (Tb.Th) (**Figure 1K**) and 19% more trabecular separation (Tb.Sp) (**Figure 1L**). This resulted in a 19% decrease in connectivity density (Conn. D.) (**Figure 1M**) and a 40% increase in the Structure Model Index (Wei et al.), which quantifies the 3D structure for the relative amount of plates (SMI=0, strong bone) and rods (SMI=3, fragile bone) (**Figure 1N**). Tibia length was unaltered (not shown).

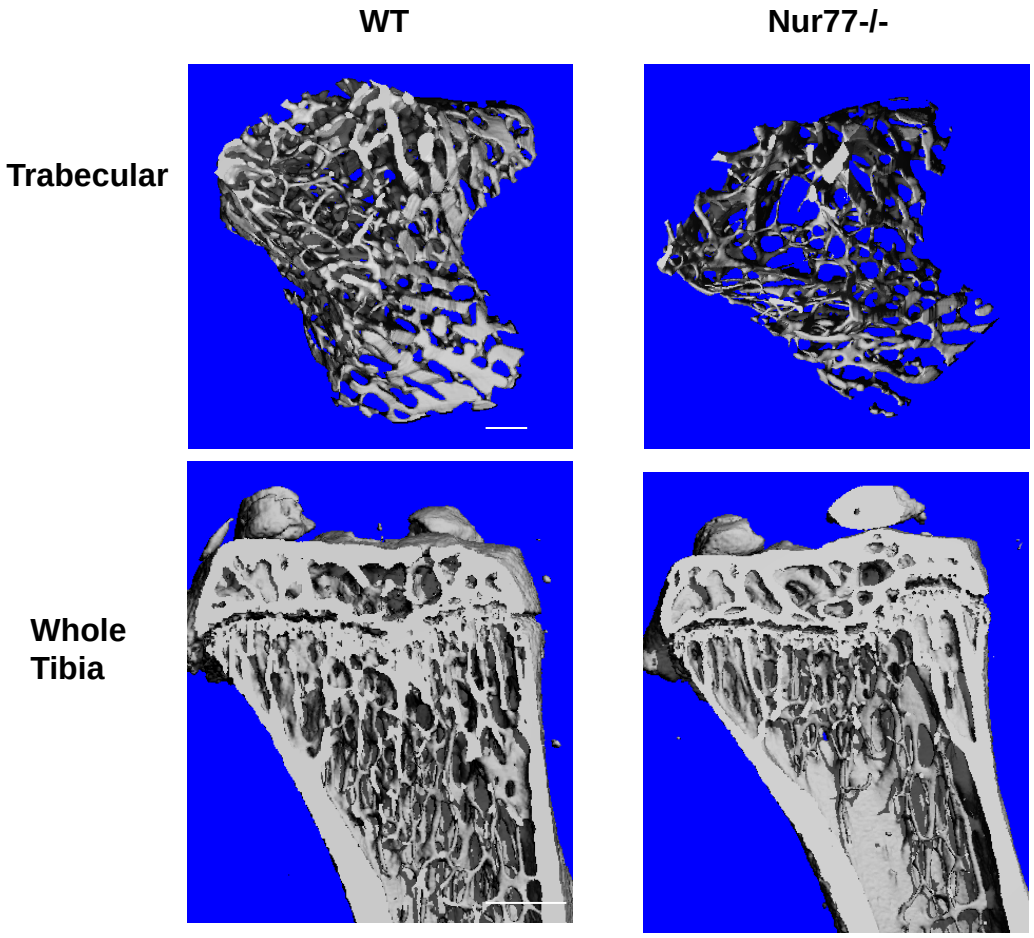

(Figure 1F) Representative images of the trabecular bone of the tibial metaphysis (scale bar, 10μm) and the entire proximal tibia (bottom) (scale bar, 1mm). Tibiae from Nur77-KO mice or WT littermate controls (2 month old, male, n=6) were analyzed by μCT.

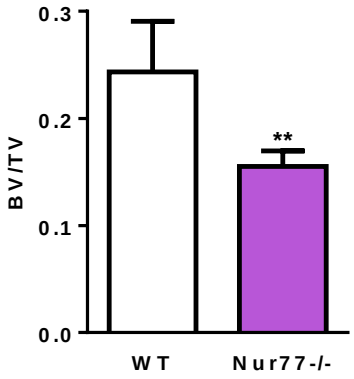
BV/TV
0.3
0.2
0.1
0.0
**
WT
Nur77-/-

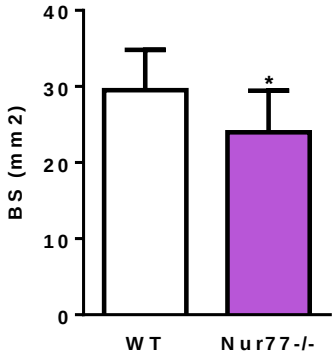
BS (mm2)
40
30
20
10
0
*
WT
Nur77-/-

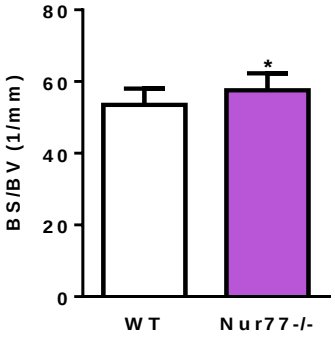
BS/BV (1/mm)
80
60
40
20
0
*
WT
Nur77-/-

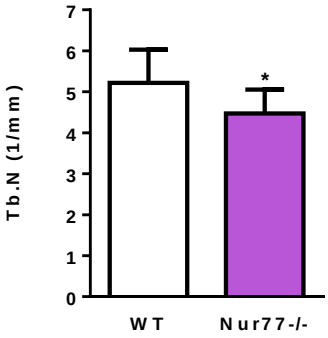
Tb.N (1/mm)
7
6
5
4
3
2
1
0
*
WT
Nur77-/-

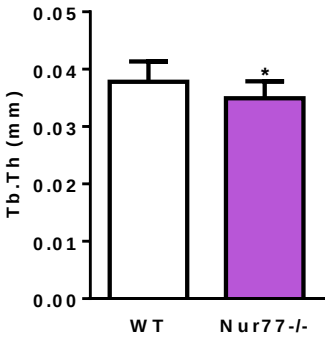
Tb.Th (mm)
0.05
0.04
0.03
0.02
0.01
0.00
*
WT
Nur77-/-

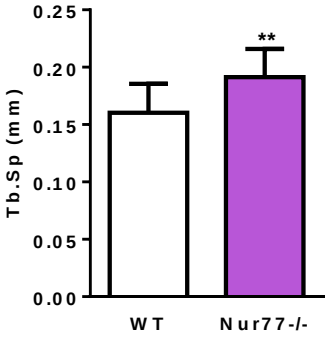
Tb.Sp (mm)
0.25
0.20
0.15
0.10
0.05
0.00
**
WT
Nur77-/-

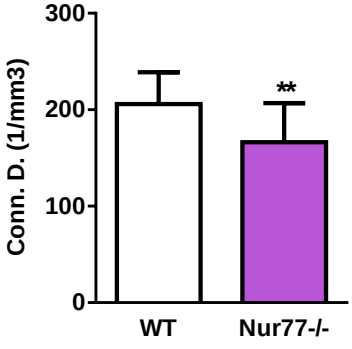
Conn. D. (1/mm3)
300
200
100
0
**
WT
Nur77-/-

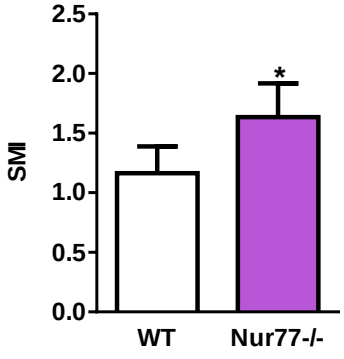
SMI
2.5
2.0
1.5
1.0
0.5
0.0
*
WT
Nur77-/-

(Figure 1G-N) Quantification of trabecular bone volume and architecture. (G) BV/TV, bone volume/tissue volume ratio. (H) BS, bone surface. (I) BS/BV, bone surface/bone volume ratio. (J) Tb.N, trabecular number. (K) Tb.Th, trabecular thickness. (L) Tb.Sp, trabecular separation. (M) Conn.D., connectivity density. (N) SMI, structure model index.

ELISA analyses showed that the serum bone resorption marker C-terminal telopeptide fragments of the type I collagen (CTX-1) was 3.7-fold higher in Nur77-KO mice (**Figure 1O**), whereas the serum bone formation marker N-terminal propeptide of type I procollagen (P1NP) was unchanged (**Figure 1P**).

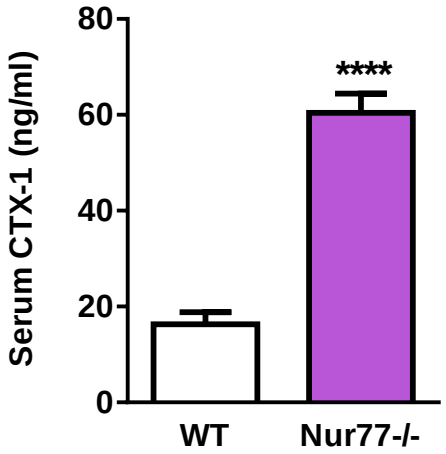

(Figure 1O) Serum CTX-1 bone resorption marker was increased (2 month old, male, n=6).

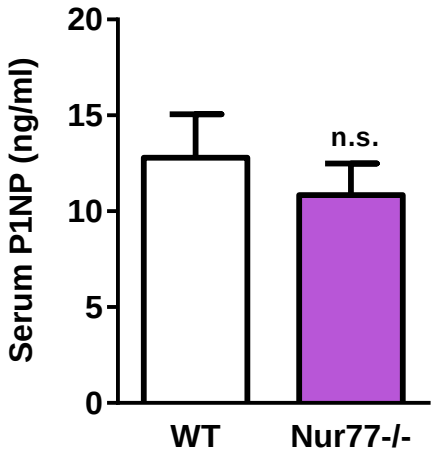

(Figure 1P) Serum P1NP bone formation marker was unaltered (2 month old, male, n=6).

Consistent with these observations, histomorphometry of the femur showed that osteoclast surface and osteoclast number were significantly increased in Nur77-KO mice (**Figure 1Q**), whereas osteoblast surface and osteoblast number (**Figure 1R**) were unaltered. Together, these results suggest that Nur77 deletion causes low bone mass primarily through increasing osteoclastogenesis and bone resorption.

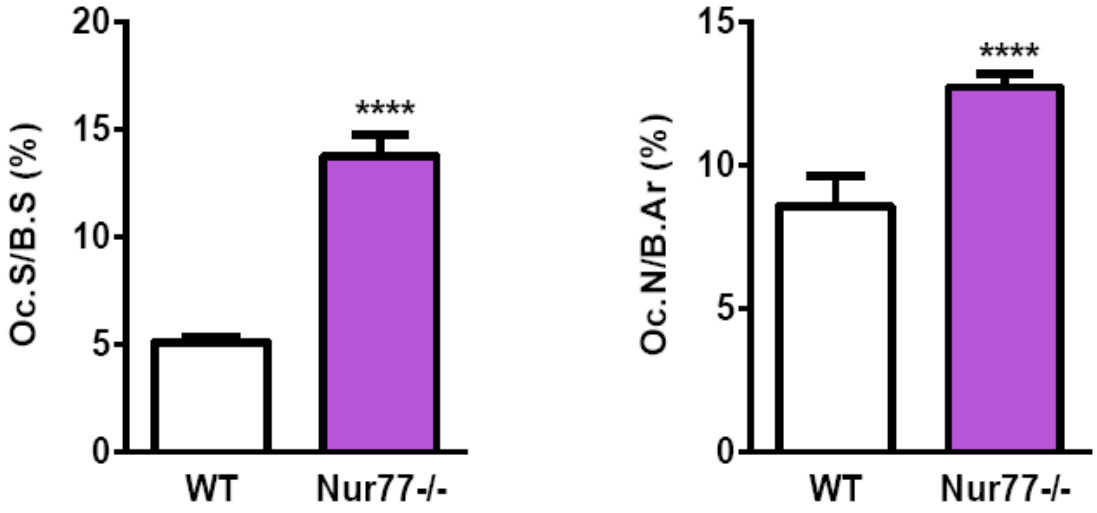

(Figure 1Q) Quantification of osteoclast surface (Oc.S/B.S) and osteoclast number (Oc.N/B.Ar).

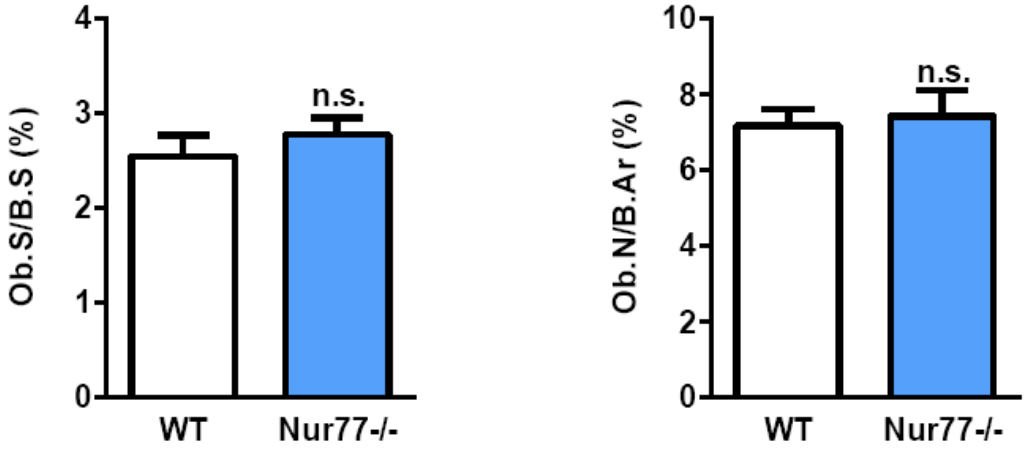

(Figure 1R) Quantification of osteoblast surface (Ob.S/B.S) and osteoblast number (Ob.N/B.Ar). B.S, bone surface; B.Ar, bone area.

Nur77 Regulation of Bone Resorption is Intrinsic to the Osteoclast Lineage

Since Nur77 has been implicated to regulate many other cell types (Hsu et al., 2004), we next performed bone marrow transplantation experiments to examine whether Nur77 regulation of bone resorption stems from the intrinsic effects in the hematopoietic/osteoclast lineage or non-autonomous effects from other tissues or cell types such as osteoblasts, osteocytes or the neuroendocrine system. Two complimentary sets of bone marrow transplantation were performed and serum bone markers were assessed two months later. In the first set, I harvested donor bone marrow cells from both WT and Nur77-KO mice, and transplanted them to irradiated WT recipient mice (**Figure 2A**). The results showed that WT mice receiving Nur77-KO bone marrow cells exhibited significantly higher CTX-1 levels than the control group (**Figure 2B**), but unaltered P1NP levels (**Figure 2C**), suggesting that Nur77-KO hematopoietic lineage was sufficient to elevate bone resorption.

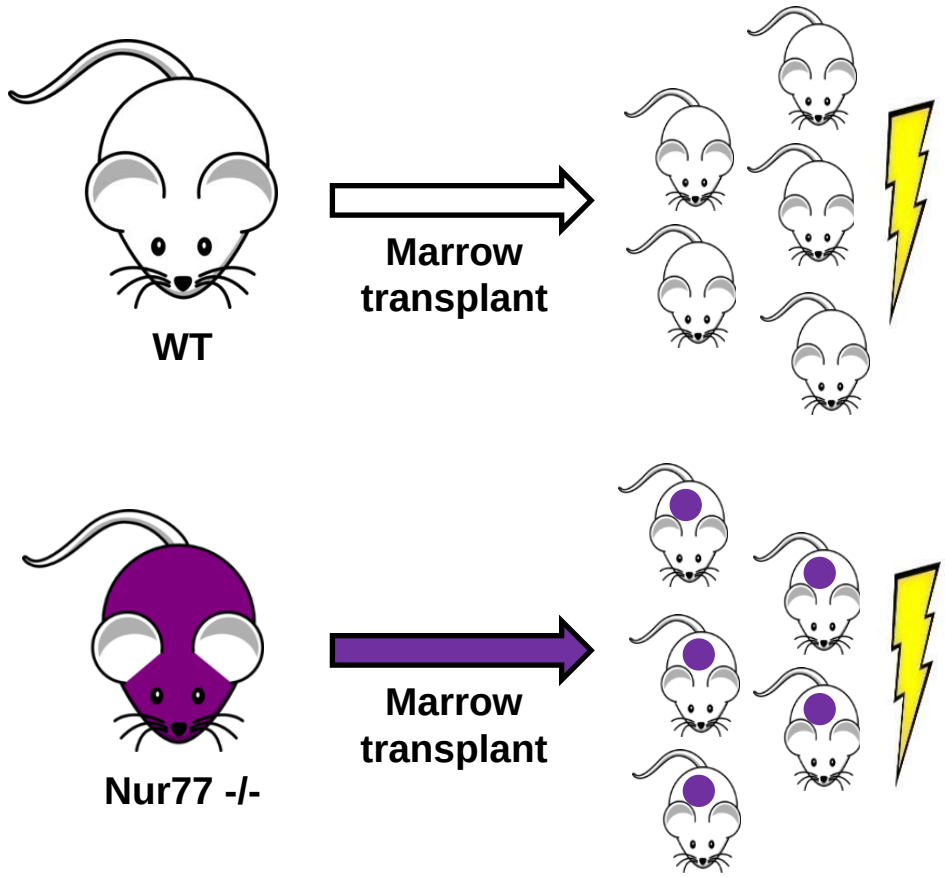

(Figure 2A) Transplantation of Nur77-KO donor bone marrow cells into WT recipients, schematic representation. 2 month old male donor and recipient, sacrificed 10 weeks after transplantation. (n=5)

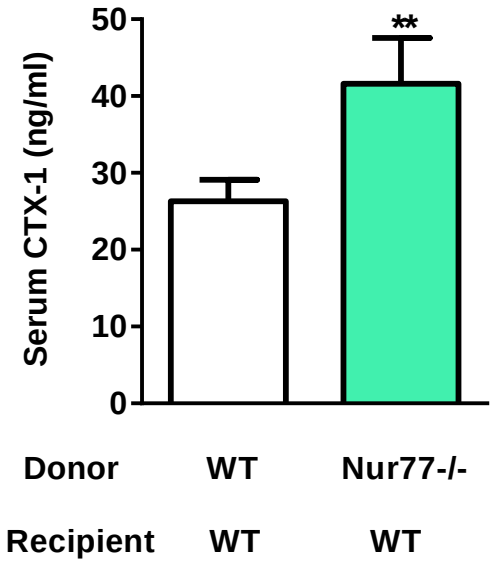

(Figure 2B). Nur77 -/- donor marrow conferred elevated bone resorption compared to WT control donor bone marrow cells, shown by Serum CTX-1. (C) Serum P1NP.

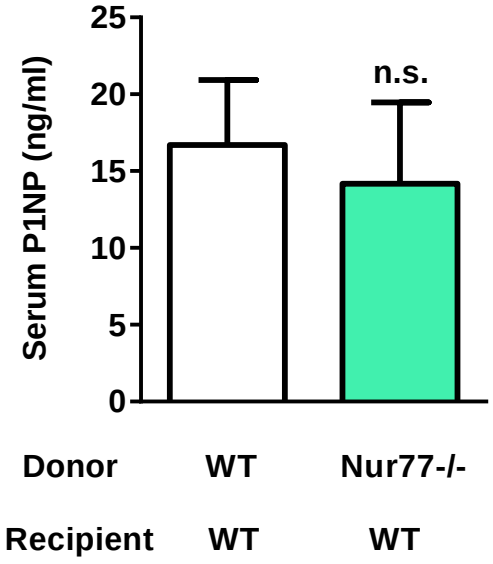

(Figure 2C). Serum P1NP

In the second set, we transplanted WT donor bone marrow cells into either Nur77-KO or WT control recipient mice (**Figure 2D**). Nur77-KO mice receiving WT bone marrow cells showed normalized CTX-1 levels similar to the control group (**Figure 2E**), with also similar P1NP levels (**Figure 2F**), suggesting that WT bone marrow can completely rescue the osteoclast defects in the Nur77-KO mice and thus other tissues/cell types play only a minor role if any. The results from these two experiments indicate that Nur77 regulation of bone resorption is intrinsic to the hematopoetic lineage.

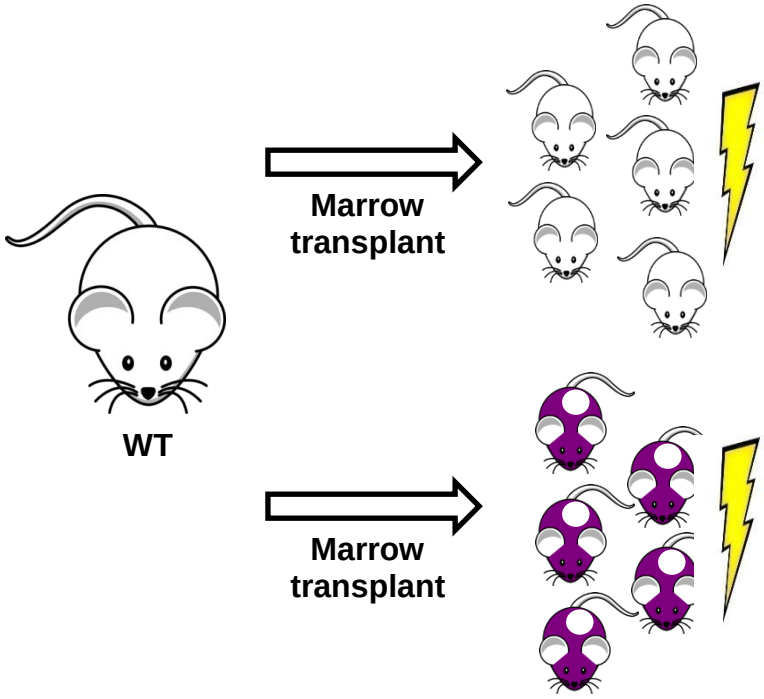

(Figure 2D) Transplantation of WT donor bone marrow cells into Nur77-KO recipients. A schematic diagram.

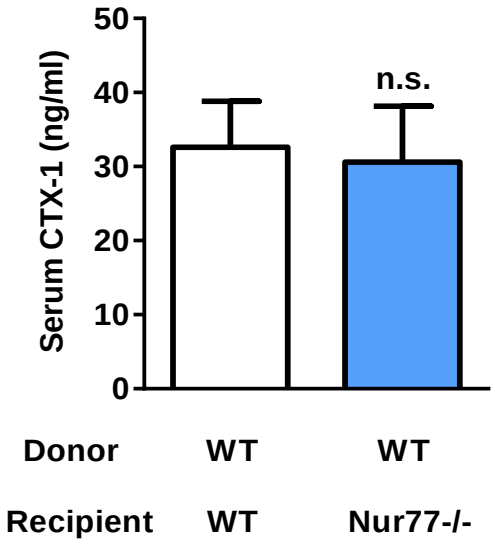

(Figure 2E) Transplantation of WT donor bone marrow cells into Nur77-KO recipients rescued the bone resorption to a level similar to the WT control recipients, as shown by serum CTX-1.

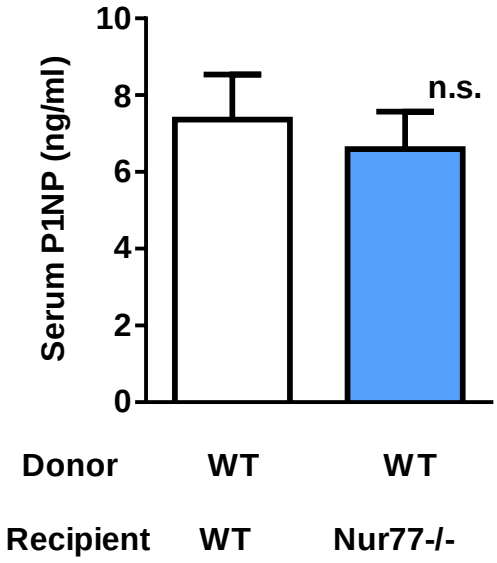

(Figure 2F) Serum P1NP.

In the bone milieu, osteoblasts and osteocytes provide RANKL and the RANKL decoy receptor OPG to stimulate and inhibit osteoclast differentiation, respectively (Boyce and Xing, 2007b). Thus, we assessed whether RANKL and OPG levels were different between Nur77-KO and WT control mice. We first compared osteoblast differentiation cultures derived from Nur77-KO or WT control mice, and found that there was no difference in the expression of RANKL or OPG, resulting in a comparable RANKL/OPG ratio (**Figure 2G**).

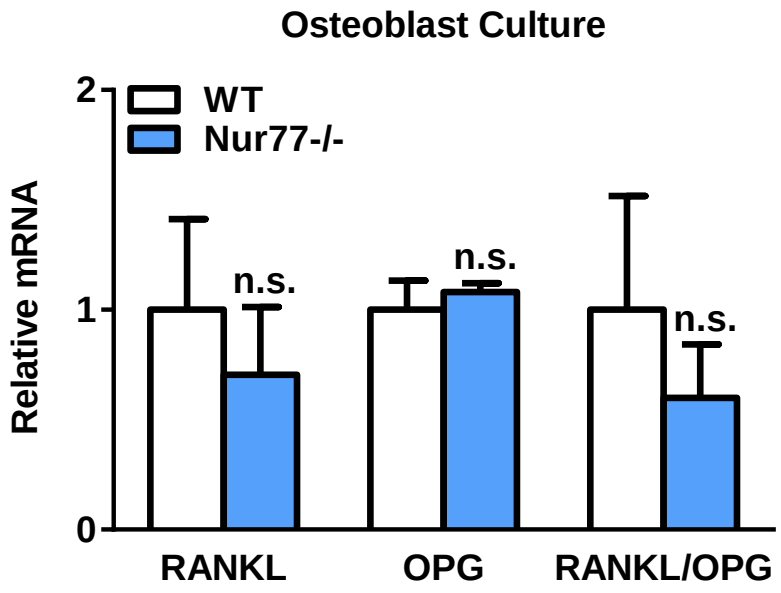

(Figure 2G) Expression of RANKL and OPG, as well as RANKL/OPG ratio, in Nur77-KO *ex vivo* osteoblast differentiation cultures compared to WT control cultures (n=3).

Recently osteocytes, the mature long living osteoblasts embedded in the bone matrix, have been shown to provide the majority of RANKL and OPG to osteoclasts (Nakashima et al., 2011; Popovic et al., 2014). Hence, we compared OPG and RANKL expression in femur shafts that contain mainly osteocytes. Our results showed that there was no difference in RANKL expression (**Figure 2H**); however, Nur77-KO osteocytes express a markedly higher level of OPG (**Figure 2H**), leading to a significantly lower RANKL/OPG ratio (**Figure 2H**). The lower RANKL/OPG ratio in the Nur77-KO mice is unlikely to be the cause of the augmented osteoclastogenesis, but presumably an attempt of osteocytes to suppress the osteoclast over-activation. These results, coupled with unaltered *in vitro* osteoblast differentiation (**Figure 1E**) and *in vivo* bone formation (**Figure 1P, R, S**), suggest that osteoblast/osteocyte are not major contributors to the excessive osteoclastogenesis and bone resorption in Nur77-KO mice.

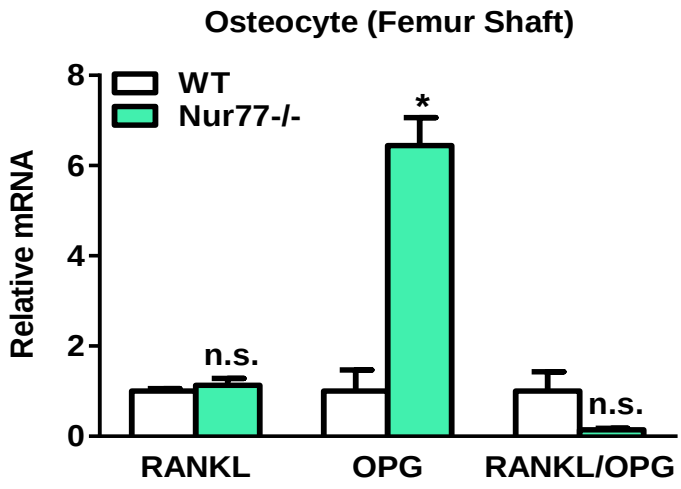

(Figure 2H) Expression of RANKL and OPG, as well as RANKL/OPG ratio, in osteocytes from femur shaft in Nur77-KO mice compared to WT control mice (n=3).

Inflammatory cytokines in the bone microenvironment can also promote osteoclast differentiation (Zupan et al., 2013). Thus, we collected bone marrow cells from mouse femurs for gene expression assessment. No significant difference was found in the expression of TNFα, IL-6 or IL1β (**Figure 2I**). Moreover, it has been shown that serum levels of TNF-a, IL-6 and IL-1 were unchanged in mice injected with either Nur77-expressing lentivirus or Nur77 siRNA (Hu et al., 2014), further suggesting that the augmented osteoclastogenesis in Nur77-KO mice is not due to differential levels of these inflammatory cytokines.

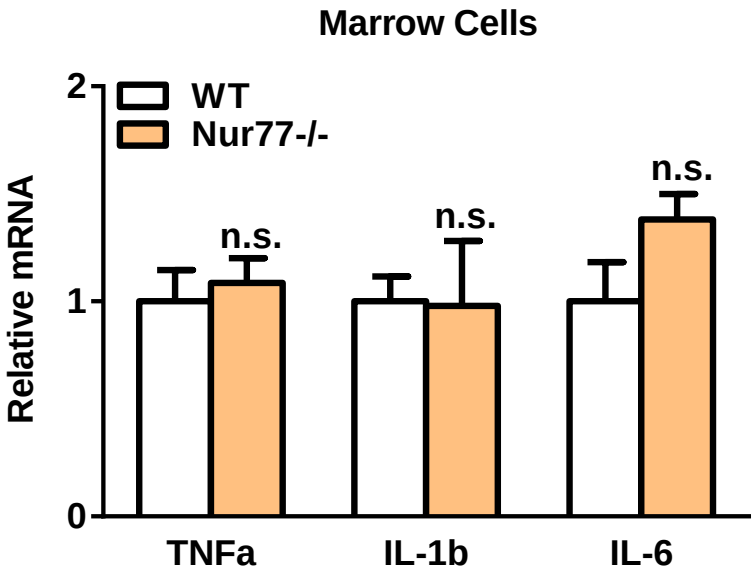

(Figure 2I) Expression of pro-osteoclastogenic cytokines in bone marrow cells from Nur77-KO mice compared to WT control mice (n=3).

The above findings, together with the fact that Nur77-KO osteoclast precursors exhibited enhanced osteoclast differentiation independent of the bone environment (**Figures 1C-D**), indicate that Nur77 regulation of osteoclastogenesis is mainly intrinsic and cell-autonomous to the osteoclast lineage.

Nur77 Promotes NFATc1 Degradation

Given that Nur77 exerts functions within the osteoclast itself, we decided to investigate whether Nur77 affects RANKL signaling pathways. RANKL binding to RANK receptor on osteoclast precursor cells activates AP1 transcription factor via c-Jun phosphorylation, as well as NFκB transcription factor via IκBα degradation, which in turn induces and initiates the autoamplification of NFATc1, the master transcriptional switch of osteoclastogenesis (Kuroda and Matsuo, 2012). Although NFATc1 mRNA level was 2-fold higher in Nur77-KO osteoclast differentiation cultures on day 3 (**Figure 1C**), I found that NFATc1 protein level was 7-fold higher in Nur77-KO cultures compared to WT control cultures on day 3 (**Figure 3A**). It has been reported that NFATc1 protein is degraded on day 3-4 during osteoclast differentiation, despite the continuously rising NFATc1 mRNA levels (Kim et al., 2010). Indeed, my time course analysis showed that in WT cultures, NFATc1 protein was elevated on day 2 but then rapidly down-regulated on day 3 and day 4 (**Figure 3A**). In contrast, in Nur77-KO cultures, the initial increase of NFATc1 protein was sustained and NFATc1 protein remained high on day 3 and day 4 (**Figure 3A**).

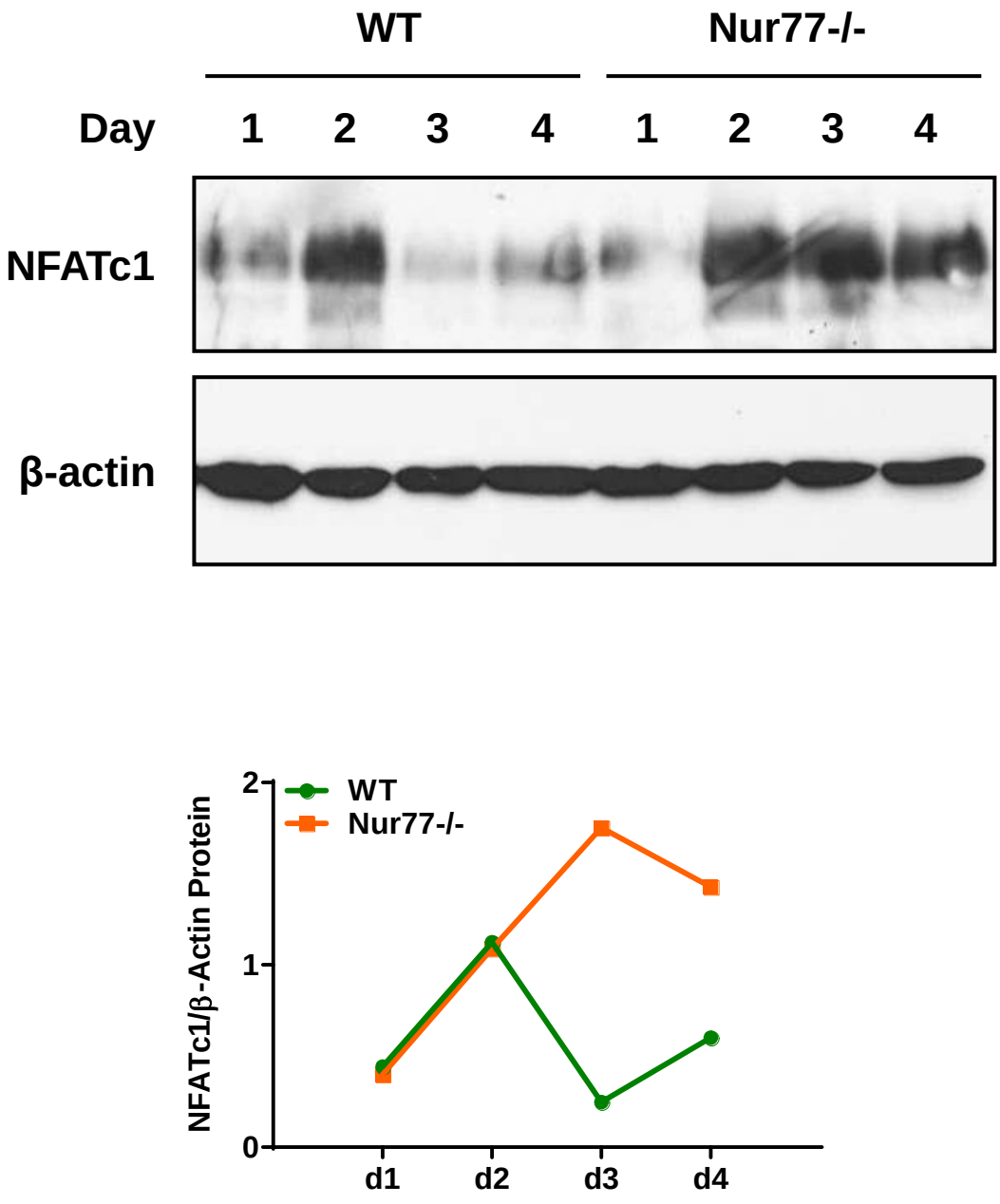

(Figure 3A) NFATc1 protein levels during a time course of osteoclast differentiation from the bone marrow cells of Nur77-KO mice or WT control mice. Top, representative western blot image. Bottom, quantification of NFATc1/β-actin ratio.

I then compared c-Jun phosphorylation and IκBα degradation in the osteoclast differentiation cultures upon RANKL stimulation, but did not observe any significant difference between Nur77-KO and WT control cultures (**Figure 3B**), which is in agreement to the similar NFATc1 protein induction on day 1 and day 2 (**Figure 3A**). This indicates that the regulation of NFATc1 protein level resides downstream of transcription.

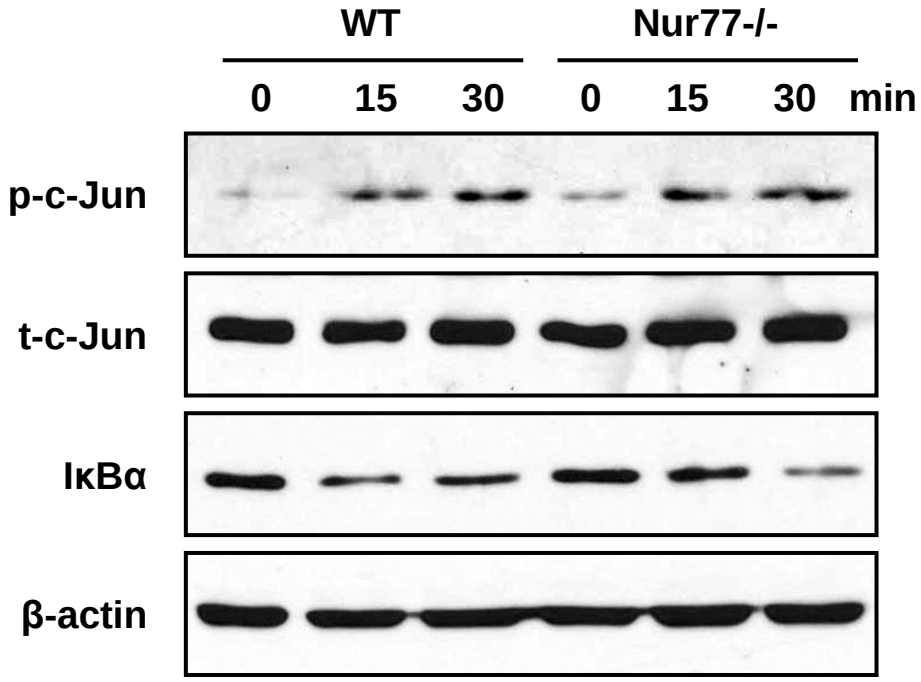

(Figure 3B) c-Jun phosphorylation and IκBα degradation post RANKL treatment in osteoclast differentiation cultures from the bone marrow cells of Nur77-KO mice or WT control mice. P-c-Jun, phosphorylated c-Jun; t-c-Jun, total c-Jun.

It has been shown that the decrease in NFATc1 protein levels at later stage of osteoclast differentiation is due to ubiquitin-mediated protein degradation; and that MG132, a proteasome inhibitor, can restore NFATc1 protein to a similar level on day 2 (Kim et al., 2010). To examine whether the differences in NFATc1 levels between Nur77-KO and WT mice were due to protein degradation, I treated osteoclast differentiation cultures with MG132 on day 3. As my result shows, MG132 treatment increased NFATc1 protein level in WT cultures to a level similar to Nur77-KO cultures; and MG132 treatment could not further increase NFATc1 protein level in the Nur77-KO cultures (**Figure 3C**). This result indicates that the ubiquitin-proteasome machinery which is responsible for degrading NFATc1 was not functional in Nur77 -/- mice. In addition, MG132 treatment equalized the NFATc1 levels between WT and Nur77 -/- mice, which suggests that the difference in protein level between WT and Nur77 -/- mice was caused by the difference in the ubiquitin pathway. As a result, I hypothesize that Nur77 deletion elevates NFATc1 protein levels by suppressing ubiquitin-degradation pathway.

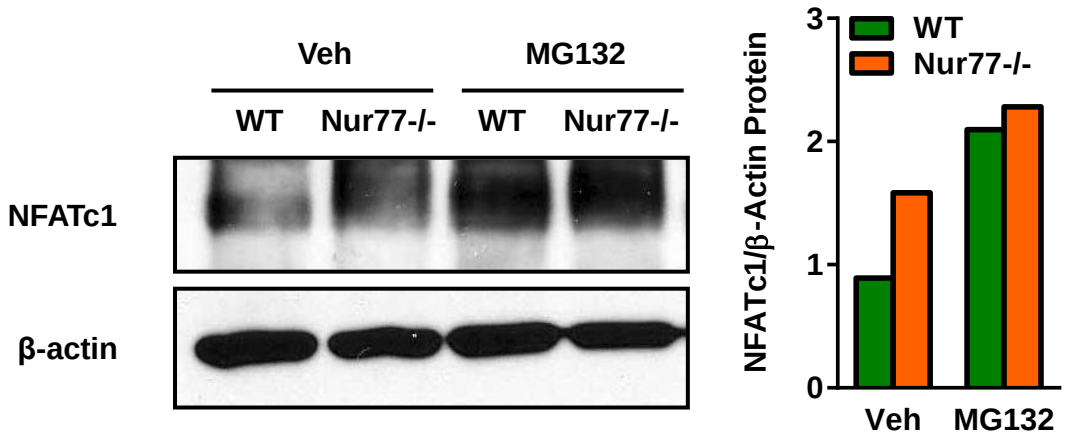

(Figure 3C) Effects of MG132 on NFATc1 protein levels in Nur77-KO or WT bone marrow osteoclast differentiation cultures. Cells were treated with 25μM MG132 for 6 hours 3 days after RANKL stimulation. Left, representative western blot image. Right, quantification of NFATc1/β-actin ratio.

As a complementary gain-of-function approach, I tested whether Nur77 over-expression could promote NFATc1 protein degradation. We transfected HEK293 cells with NFATc1 together with Nur77 or a GFP control, and then quantified NFATc1 mRNA and protein levels. The result shows that Nur77 over-expression significantly decreased NFATc1 protein levels (**Figure 3D, Top**) without altering NFATc1 mRNA levels (**Figure 3D, Bottom**).

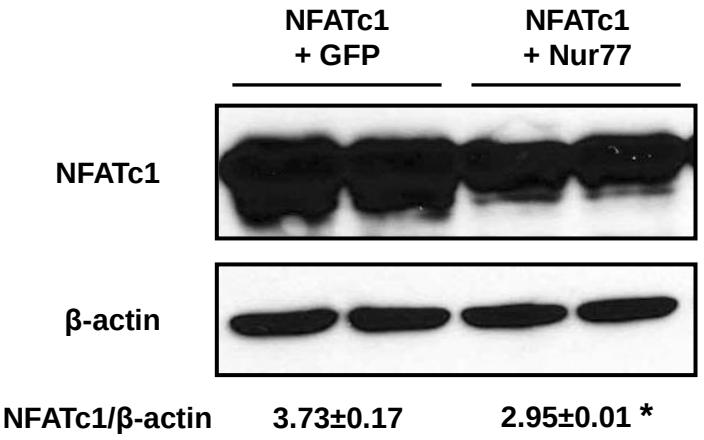

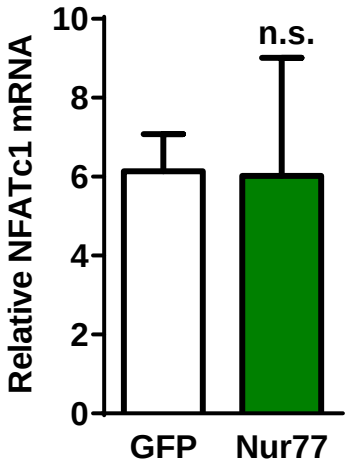

(Figure 3D) Effects of Nur77 over-expression on NFATc1 protein and mRNA levels. HEK293 cells were transfected with NFATc1, together with either Flag-Nur77 or GFP control. Top, representative western blot image with quantification of NFATc1/β-actin ratio. Bottom, relative NFATc1 mRNA.

Consistent with the lower Nur77 protein abundance, Nur77 over-expression also dosage-dependently reduced the NFATc1 transcriptional output from a luciferase reporter driven by NFATc1 response elements (**Figure 3E**). These findings further support the notion that Nur77 promotes NFATc1 protein degradation.

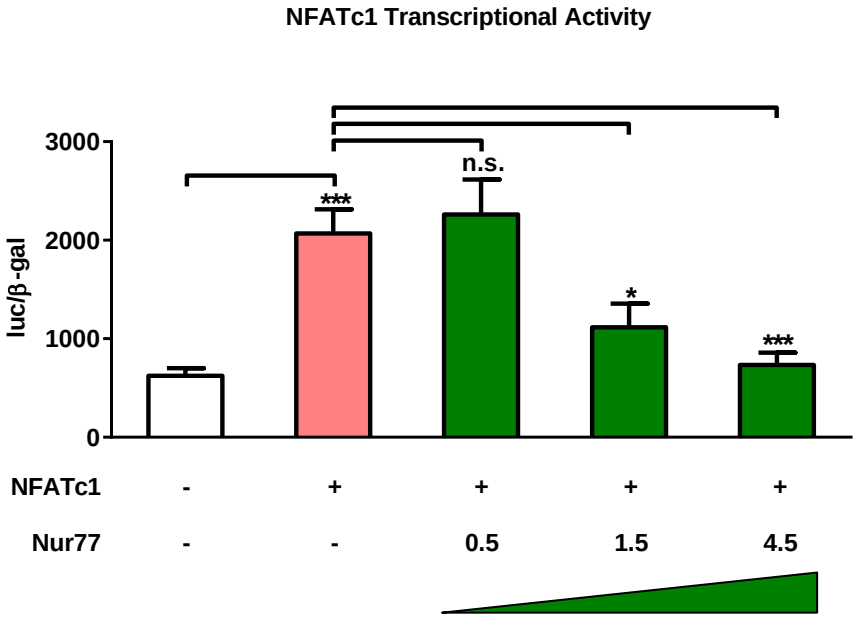

(Figure 3E) Effects of Nur77 over-expression on NFATc1 transcriptional output. HEK293 cells were transfected with NFATc1 and its luciferase reporter, together with increasing amount of Nur77.

Given that Nur77 can decrease NFATc1 protein level, hypothesized that Nur77 can physically interact with NFATc1 to modulate its stability. As a result, I performed a co-immunoprecipitation experiment to see if Flag-Nur77 can bind to NFATc1. My results **(Figure 3F)** showed that by using either Flag or NFATc1 antibody, I can not pull down NFATc1 or Nur77, which suggest that these two do not directly interact. Hence, it is more likely that Nur77 regulate another protein that modulates NFATc1 stability.

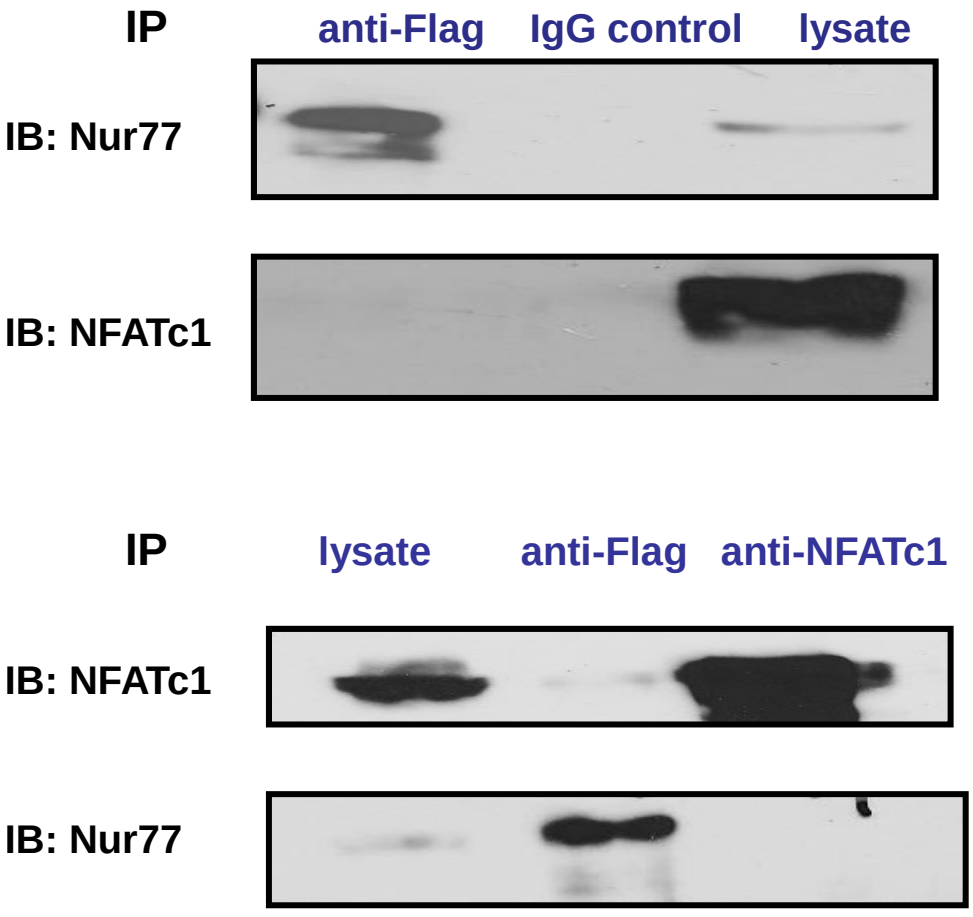

(Figure 3F) Co-immunoprecipiation of NFATc1 and Nur77

Nur77 transcriptionally up-regulates E3 ligase Cbl-b

In the ubiquitin degradation pathway, E3 ligases are responsible for substrate specificity and ubiquitination regulation. We next searched for E3 ligases that could be responsible for NFATc1 degradation in osteoclasts. It has been reported that Cbl-b, an E3 ligase in the Cbl family, is a major contributor to the ubiquitin-mediated down-regulation of NFATc1 at late stage of osteoclast differentiation (Kim et al., 2010). Cbl family contains proteins Cbl-b, Cbl and Cbl-3 proteins, but only Cbl and Cbl-b are abundantly expressed in osteoclasts and other hematopoietic cells. (Nakajima et al., 2009) Therefore, we tested the hypothesis that Nur77 may promote NFATc1 degradation by inducing Cbl-b, Cbl or both. We found that Cbl-b expression was significantly lower in Nur77-KO osteoclast differentiation cultures compared to WT control cultures on day 2 and day 4 (**Figure 4A**), while Cbl levels were comparable between Nur77 WT and KO mice (data not shown).

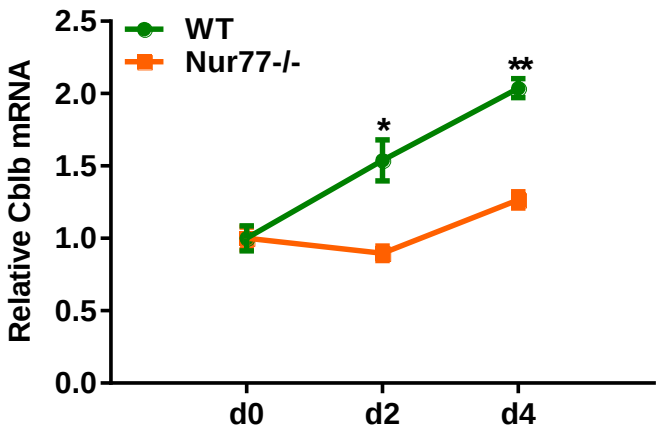

(Figure 4A) Cbl-b expression during a time course of osteoclast differentiation from the bone marrow cells of Nur77-KO mice or WT control mice (n=3).

Conversely, Nur77 over-expression in HEK293 cells significantly increased Cbl-b expression (**Figure 4B**), but not Cbl levels (data not shown). Importantly, a truncated Nur77 mutant in which the DNA binding domain (DBD) was deleted could no longer up-regulate Cbl-b, suggesting that Nur77 induction of Cbl-b transcription depends on its DNA binding ability (**Figure 4B**). The functional connection between Nur77 and Cbl-b is further supported by the similar bone phenotype in Nur77-KO mice (**Figure 1**) and Cbl-b-KO mice (Nakajima et al., 2009), including increased *ex vivo* osteoclast differentiation and *in vivo* bone resorption, but unaltered bone formation, leading to lower bone mass. By contrast, Cbl knock-out mice had no apparent bone phenotype in adult mice, and only exhibited modest impairment in osteoclast motility in embryonic bone development.

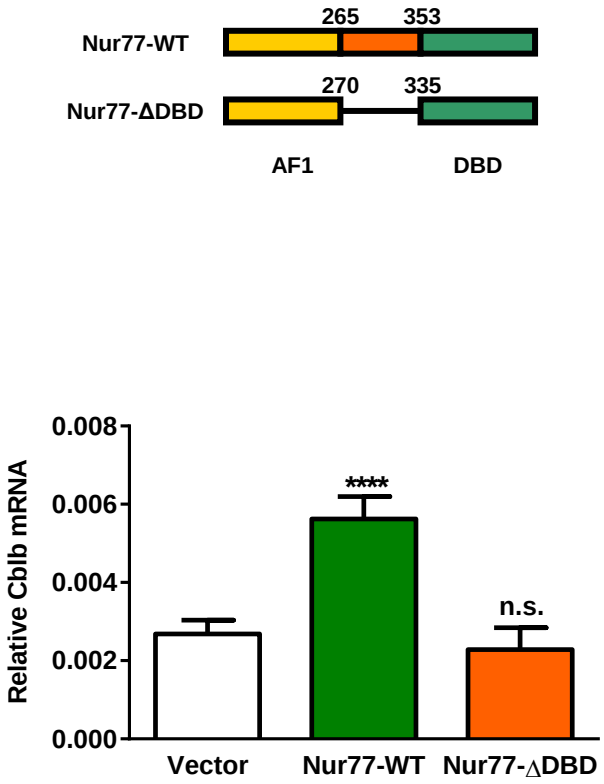

(Figure 4B) Nur77 over-expression increased Cbl-b mRNA in a DNA-binding-dependent manner. HEK293 cells were transfected with vector control, WT Nur77 or a mutant Nur77 with a deletion of the DNA binding domain (DBD) (n=3).

To investigate whether Cbl-b is a direct Nur77 target gene, I tested whether Nur77 could transcriptionally activate the Cbl-b promoter. O cloned a 1kb segment of Cbl-b promoter upstream of a luciferase reporter and tested its expression in a transient transfection assay in HEK293 cells. The result showed that co-transfection with Nur77 significantly up-regulated the Cbl-b promoter activity by 2.2-fold (**Figure 4C**), suggesting that Nur77 is able to directly activate Cbl-b transcription. Bioinformatic analyses revealed a pair of motifs that may comprise a Nur77 response element (NurRE) in the Cbl-b promoter at ~600bp upstream of the transcription start site (**Figure 4C, inset**). By contrast, I didn't find NurRE in Cbl promoter, further confirming that Cbl-b is the major functional target of Nur77 in osteoclastogenesis.

To examine whether these putative NurRE motifs are important for Nur77 induction of Cbl-b promoter, I mutated each NurRE motif to derive mutant-1 and mutant-2 luciferase reporters (**Figure 4C, inset**). Although not completely abolishing Nur77' effect, both mutant reporters exhibited a significantly compromised ability to be activated by Nur77 compared to the WT reporter (**Figure 4C**), indicating that both NurRE motifs are functionally required. The residual activity could be due to incomplete mutation of the regulatory element, or other elements that has yet to be identified.

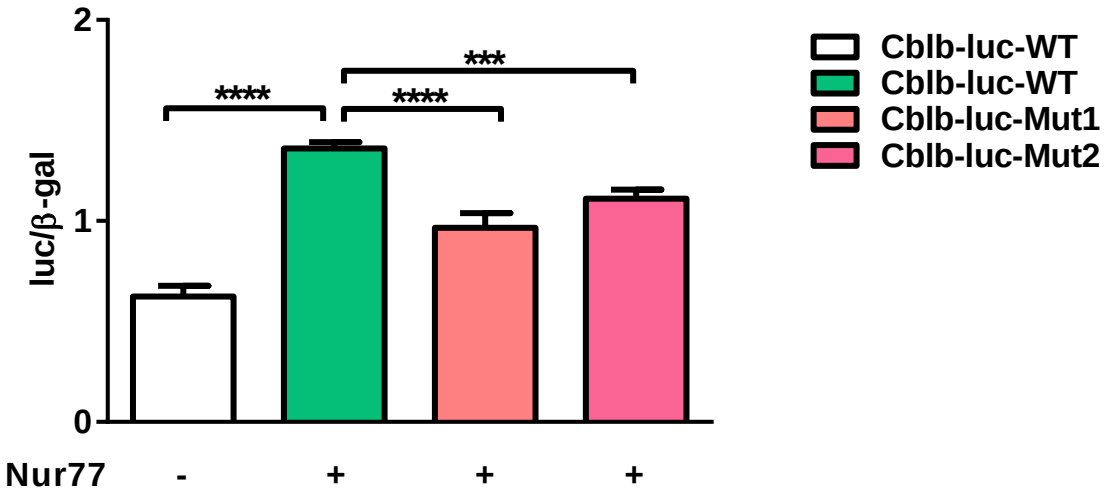

WT AAATATCAgaacatcTGAGATGA

Mut1 AACCAGCAgaacatcTGAGATGA

Mut2 AAATATCAgaacatcTGCGACGC

(Figure 4C) Nur77 activated Cbl-b promoter via NurRE. HEK293 cells were transfected with Nur77, together with a luciferase vector control or a luciferase reporter driven by 1Kb Cbl-b promoter containing either a WT NurRE or a mutant NurRE (n=3). Inset shows the mutations in the two mutant reporters.

To determine whether Nur77 can bind to the endogenous Cbl-b NurRE, we performed Chromatin Immunoprecipitation (ChIP) assay. Nur77 was found to be enriched at the NurRE region, leading to transcription activation shown by the presence of H3K4Me3 histone mark at the transcription start site (**Figure 4D**). These results suggest that Nur77 can directly induce Cbl-b transcription by binding to a NurRE in the Cbl-b promoter.

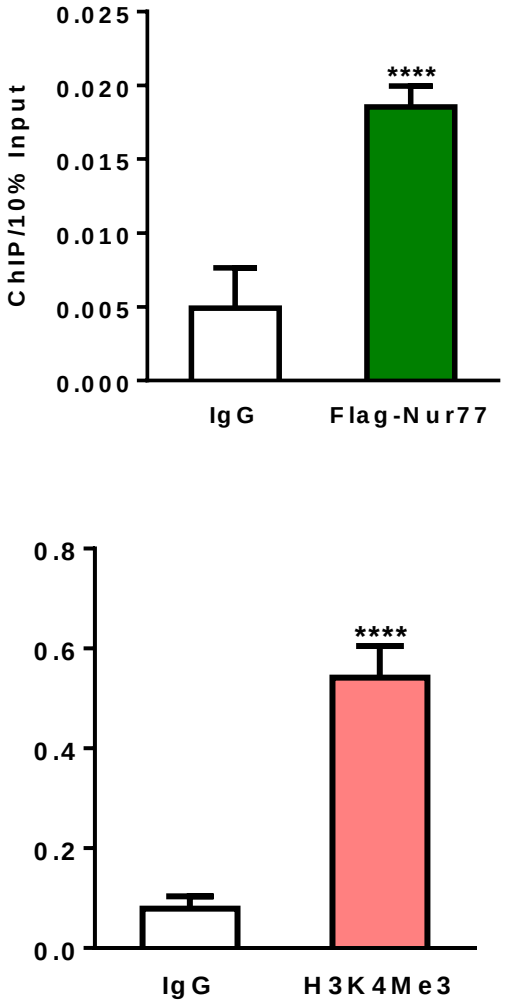

(Figure 4D) ChIP assay of Nur77 binding and H3K4me3 levels at the endogenous Cbl-b promoter. HEK293 cells were transfected with Flag-Nur77, Nur77 binding were detected with anti-Flag antibody and compared with IgG control antibody (n=3).

I next sought to elucidate whether Nur77 induction of Cbl-b is functionally required for Nur77 down-regulation of NFATc1 protein. Instead of deleting Cbl-b, we designed a more prudent strategy to specifically disrupt the NurRE region in the endogenous Cbl-b promoter using CRSPR/Cas9 genome editing tool, thus more precisely dissecting the functional interaction among Nur77, Cbl-b and NFATc1 (**Figure 4E**). Compared with WT control cells, the ability of Nur77 to increase Cbl-b mRNA (**Figure 4F**), was significantly attenuated in two indpendenet CRISPR mutant clones. This results not only confirms that Nur77 transcriptionally up-regulate Cbl-b expression, but also established the NurRE we identified through previous mutagenesis assay to be the key regulatory element through which Nur77 activates Cbl-b promoter.

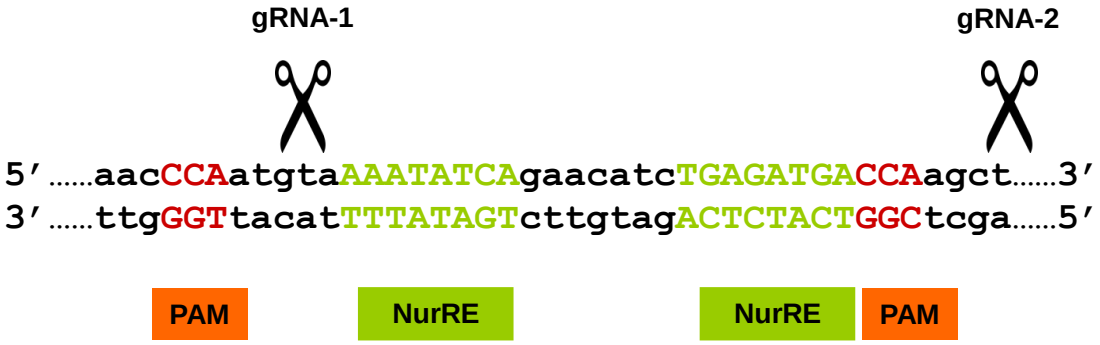

(Figure 4E) A schematic representation of CRISPR/Cas9 gRNAs and their target locus in the Cbl-b promoter.

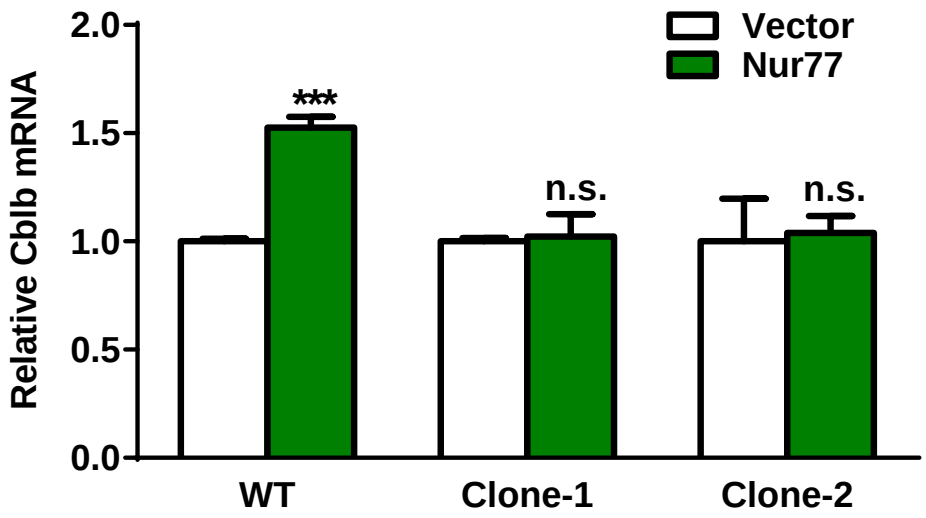

(Figure 4F) Effects of Nur77 over-expression on Cbl-b mRNA (n=4)

To establish the functional role of NurRE deletion of Cbl-b promoter in Nur77's regulation of NFATc1, I tested the NFATc1 protein level and transcriptional output in WT and mutant CRISPR clones. My result showed that NurRE deletion, and resulting attenuated Cbl-b up-regulation, significantly decreased Nur77's ability to down-regulated NFATc1 protein level **(Figure 4G)** and transitional activity **(Figure 4H).** These results provide strong evidence that Nur77 promotes NFATc1 protein degradation by directly inducing the transcription of Cbl-b E3 ligase.

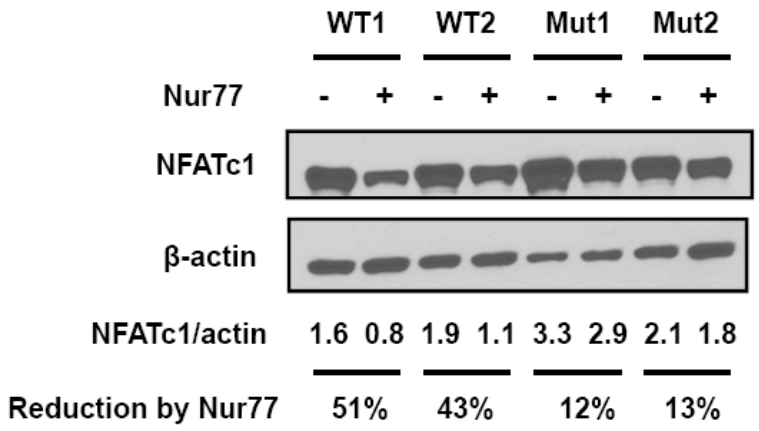

(Figure 4G) Effects of Nur77 over-expression on NFATc1 protein

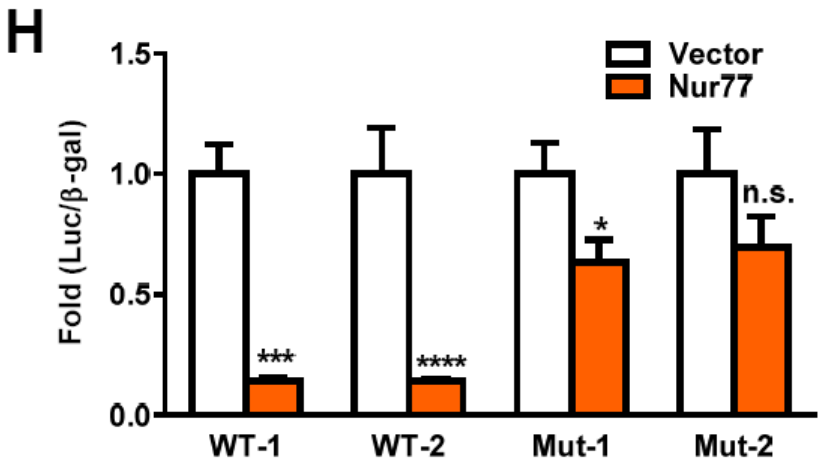

(Figure 4H) Effects of Nur77 over-expression on NFATc1 transcriptional output.

Cbl-b Confers Nur77's Regulation of Osteoclast *In Vivo*

To further assess whether Nur77 regulate osteoclastogenesis though Cbl-b, I bred both Nur77 -/- and Cblb -/- mice to create double knock-out mice, and compared osteoclast differentiation in Nur77 +/+, Nur77 -/-, Cbl-b -/- Nur77 +/+ and Cbl-b -/- Nur77 -/- mice. TRAP staining showed that while Nur77 -/- mice have marked higher degree of osteoclast differentiation than WT, Nur77 loss no longer has an effect on osteoclast on a Cbl-b null background **(Figure 5A).** qPCR quantification of CTSK **(Figure 5B)** and TRAP **(Figure 5C)** expression also confirmed the same observation. These data utilized powerful in vivo model to

confirm the functional link between Nur77 and Cbl-b in mouse osteoclast development, but also supported our hypothesis that compared with c-Cbl, Cbl-b confers the majority of Nur77's regulation on osteoclast. This does not deny that c-Cbl might have some role in other aspects of osteoclast development, but in the context of Nur77 regulation, I believe Cbl-b is the major target.

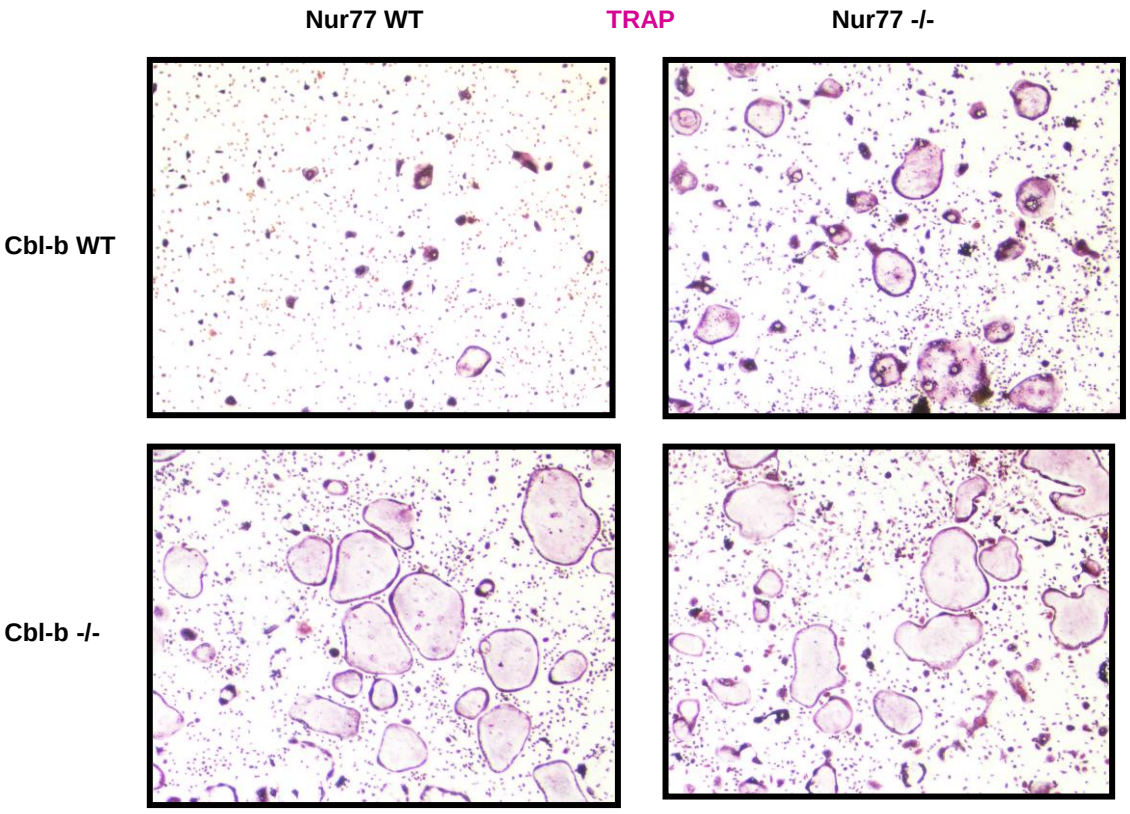

(Figure 5A) Representative images of osteoclast TRAP staining from 2 month old mice.

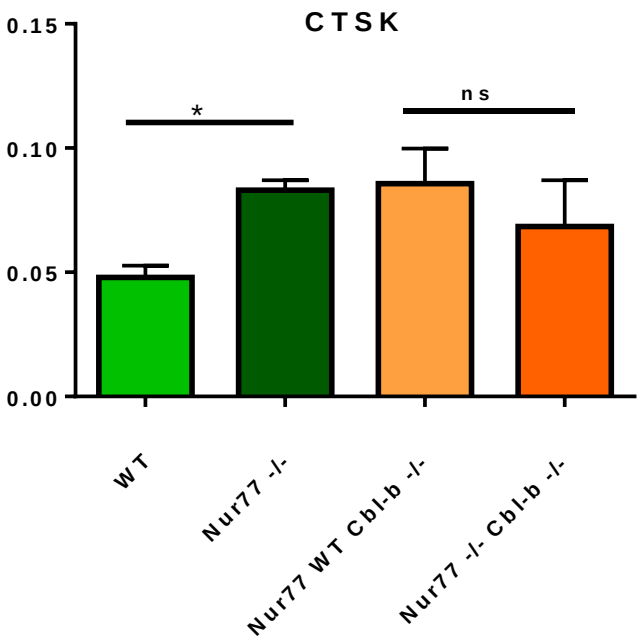

(Figure 5B) CTSK level in 2 month old male mice. (n=4)

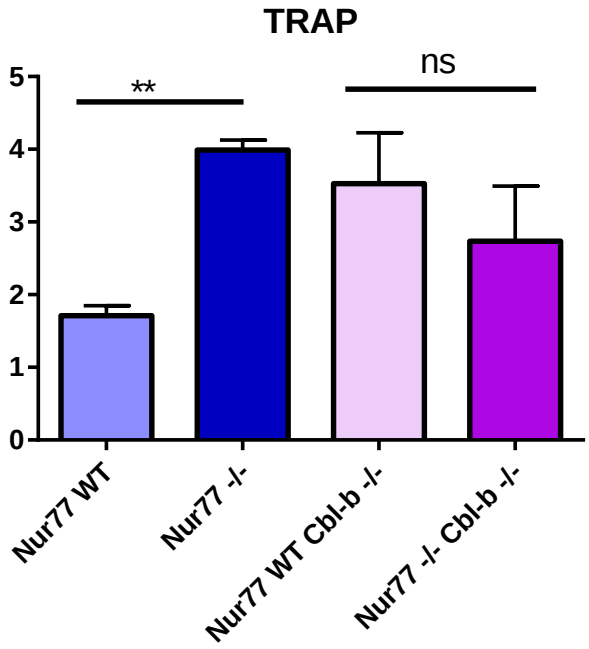

(Figure 5C) TRAP level in 2 month old male mice. (n=4)

NFATc1 Up-regulates Nur77 to Form a Self-limiting Loop

Since Nur77 expression consistently rises during osteoclastogenesis (**Figure 1B**), we hypothesize that there is an upstream regulator that induces Nur77 transcription upon RANKL signaling activation. Interestingly, we found several NFATc1 response elements in the Nur77 promoter region, suggesting that NFATc1 up-regulates Nur77 to initiate a negative feedback loop. To test whether NFATc1 itself is sufficient to increase Nur77 expression independent of other RANKL signaling pathways, we performed transfection assays to over-express NFATc1. Compared to a GFP negative control, NFATc1 over-expression significantly increased Nur77 expression in both HEK293 cells and mouse myoblast C2C12 cells (**Figure 6A**). Conversely, treatment of osteoclast differentiation cultures with cyclosporin A, a calcineurin inhibitor that suppresses NFATc1 activity, dosage-dependently decreased Nur77 expression (**Figure 6B**).

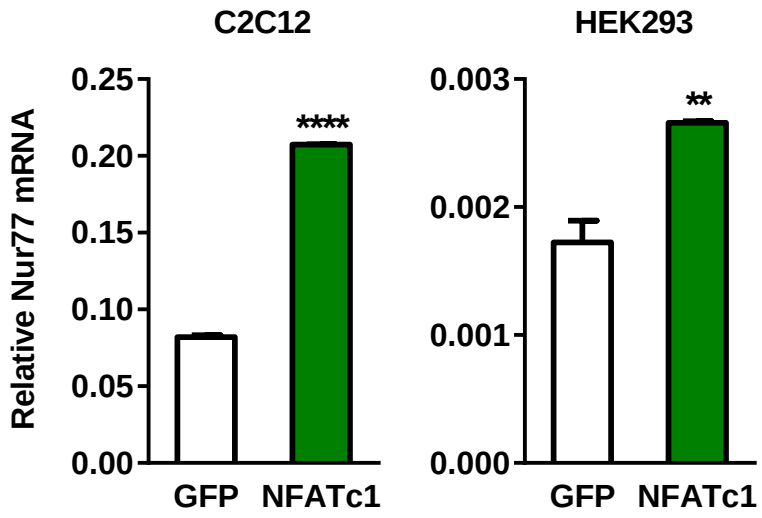

(Figure 6A) NFATc1 over-expression increased Nur77 mRNA. Mouse myoblast cell line C2C12 or human embryonic kidney cell line HEK293 were transfected with NFATc1 or GFP control.

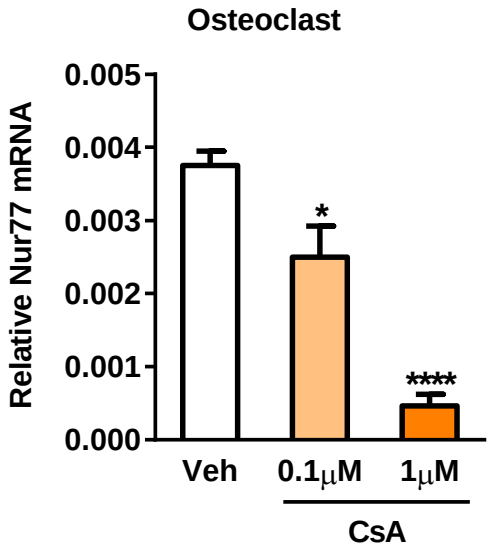

(Figure 6B) NFATc1 inhibition by Cyclosporin A dosage-dependently decreased Nur77 mRNA. Osteoclast differentiation cultures were treated with Cyclosporin A on day 2 for 24 hours (n=4).

We next examined whether NFATc1 could directly activate Nur77 promoter. We cloned a 0.8Kb Nur77 promoter region upstream of a luciferase reporter and tested its inducibility by NFATc1 by transient transfection. Compared to a GFP negative control, NFATc1 over-expression significantly elevated the luciferase output (**Figure 6C**). Moreover, ChIP assay showed that RANKL treatment of osteoclast differentiation cultures markedly increased NFATc1 binding to the endogenous Nur77 promoter (**Figure 5D**), leading to activated Nur77 transcription as shown by the higher level of H3K4Me3 histone mark at the transcription start site (**Figure 5D**).

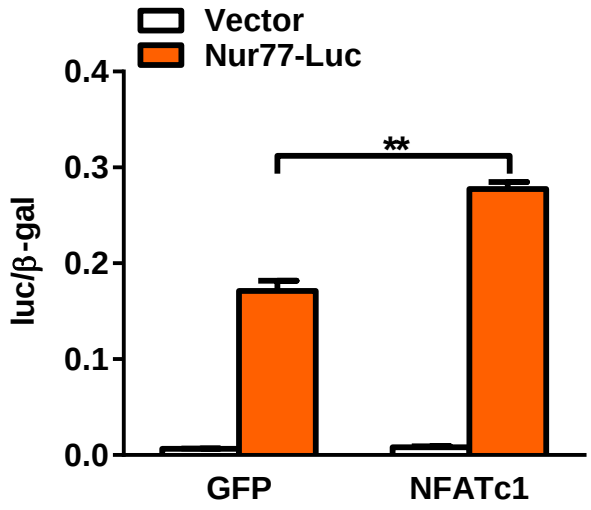

(Figure 6C) NFATc1 over-expression enhances Nur77 promoter activity. HEK293 cells were transfected with a luciferase vector control or a luciferase reporter driven by a 0.8Kb Nur77 promoter, together with NFATc1 or GFP control (n=3).

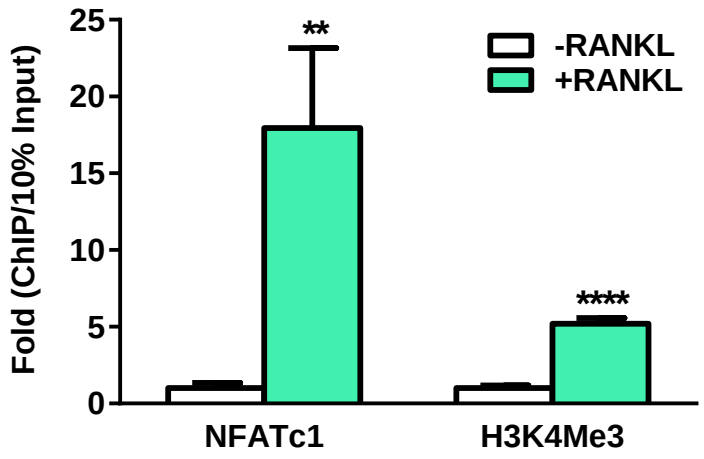

(Figure 6D) ChIP assay of NFATc1 binding and H3K4me3 level at the endogenous Nur77 promoter in RAW264.7 mouse macrophage cell line with or without 2 day RANKL stimulation.

Together, these results indicate that Nur77 is a direct transcriptional target of NFATc1, and thus revealing a key mechanism for how NFATc1 resolves its own signaling to prevent excessive osteoclastogenesis via an NFATc1→Nur77→Cblb—•NFATc1 self-limiting loop (**Figure 6E**).

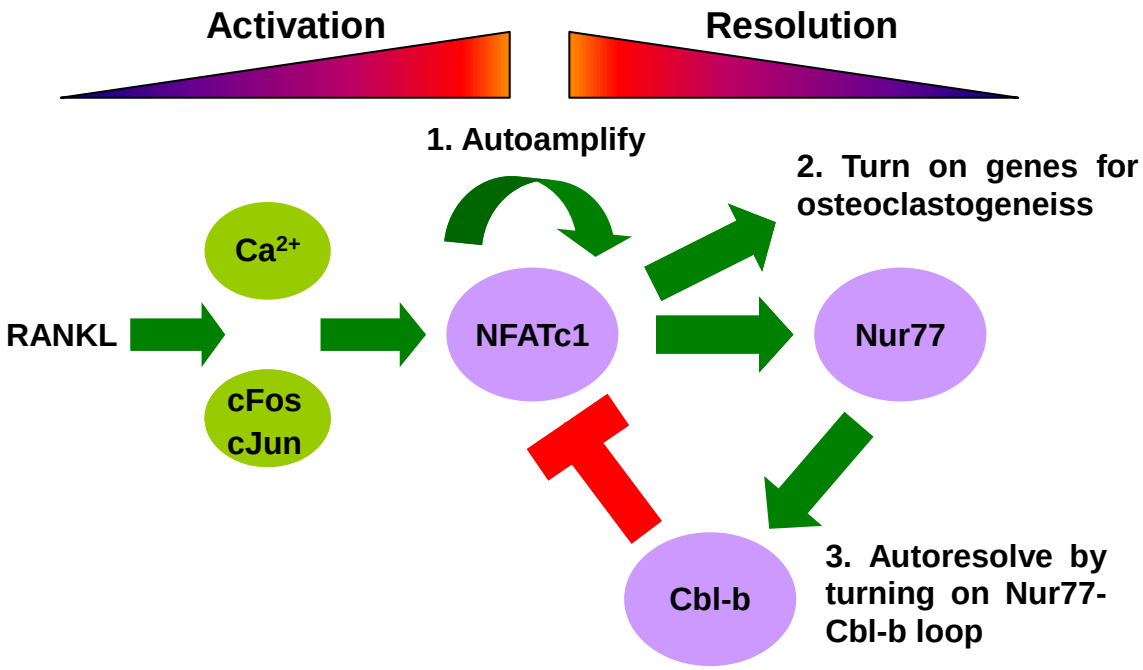

(Figure 6E) A working model of an NFATc1 self-limiting loop in which NFATc1 elicits its own degradation by inducing Nur77 and Cbl-b to resolve NFATc1 signaling.

Lower Nur77 Levels Correlate with Human Skeletal Diseases

To explore whether the critical role of Nur77 in bone remodeling translates to human skeletal biology, we analyzed NIH GEO databases to compare Nur77 expression in patients with skeletal disorders vs. healthy controls. We found that Nur77 level in bone callus tissue was significantly diminished in patients with non-union skeletal fracture than patients with normal fracture healing (**Figure 7A**). Nurr1 and NOR1 levels were also markedly reduced in patients with non-union fractures, although their expression was much lower than Nur77 (**Figure 7A**), reinforcing that Nur77 is the dominant regulator in the NR4A family during bone remodeling. Successful fracture healing depends on tightly orchestrated temporal and spatial distribution and activation of osteoclast and osteoblast (Schell et al., 2006). Given that loss of Nur77 causes elevated osteoclast activity and unaltered osteoblast activity, it is possible that the non-union healing in these patients is due to excessive bone resorption.

Furthermore, the level of Nur77, but not Nurr1 or NOR1, in the synovial tissues was also significantly lower in patients with rheumatoid arthritis than normal controls (**Figure 7B**). Given the known association of rheumatoid arthritis with elevated osteoclast activity (Hirayama et al., 2002), it's possible that the increased bone resorption is partially attributed to the compromised Nur77 expression in these patients.

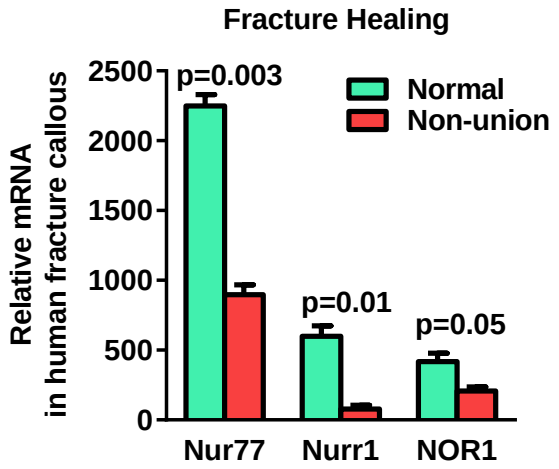

(Figure 7A) Expression of Nur77, Nurr1 and NOR1 in bone callous from patients with non-union fracture healing (fracture not healed after 6 months) vs. patients with normal fracture healing (n=5).

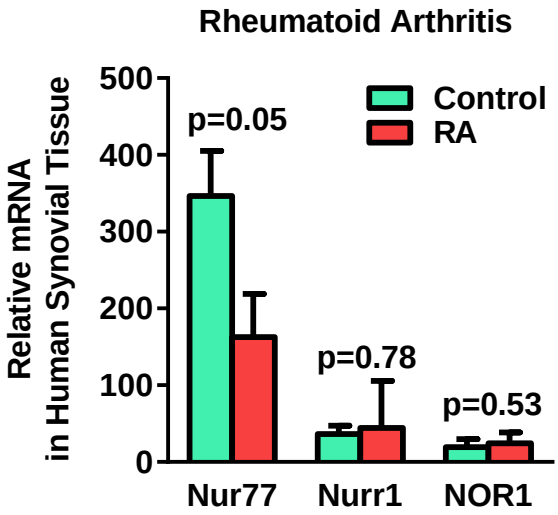

(Figure 7B) Expression of Nur77, Nurr1 and NOR1 in synovial tissue from patients with rheumatoid arthritis (RA) vs. normal controls (n=5).

Interestingly, we found that Cbl-b and Nur77 exhibit similar changes in expression in these skeletal disorders. Like Nur77, Cbl-b levels were also considerably lower in patients with either non-union fractures (**Figure 7C**) or rheumatoid arthritis (**Figure 7D**) compared with the corresponding controls. These data further support the positive functional link between Nur77 and Cbl-b. Importantly, the level of Cbl was unaltered in these patients (**Figure 7C-D**), indicating that Cbl-b is the dominant Cbl family member that regulates skeletal homeostasis in response to Nur77.

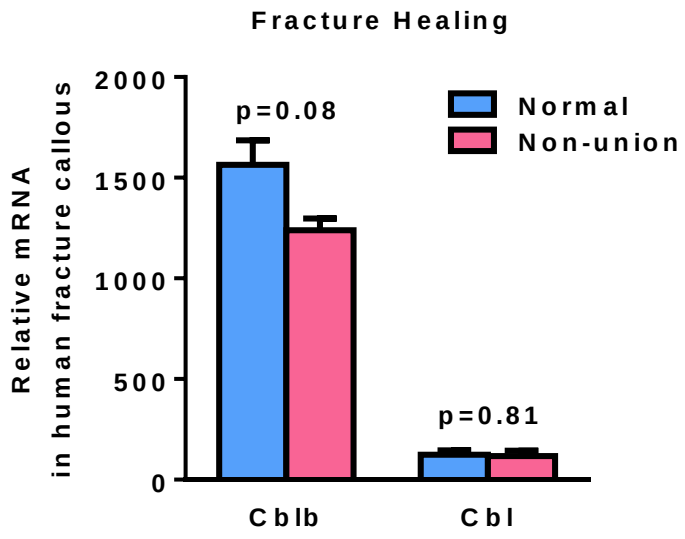

(Figure 7C) Expression of Cbl-b and Cbl in bone callous from patients with non-union fracture healing (fracture not healed after 6 months) vs. patients with normal fracture healing (n=5).

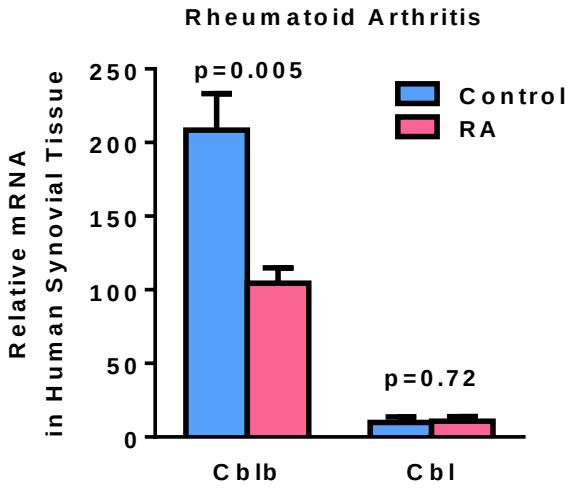

(Figure 7D) Expression of Cbl-b and Cbl in synovial tissue from patients with rheumatoid arthritis (RA) vs. normal controls (n=5). Data were retrieved from NIH GEO databases.

Finally, recent studies suggested that cancer bone metastasis to the bone to is correlated with osteoclast activity (Azim and Azim, 2013). Since our Nur77 KO mice has higher bone resorbing activity, I hypothesized that Nur77 KO will have higher bone metastasis than WT. To study how Nur77 loss affects bone metastasis, I employed 2 different mouse models. The first is to inject B16-F10 mouse melanoma

cells to WT and Nur77 -/- mice, and compare metastasis level by bioluminescence reading. Both WT and Nur77 -/- had comparable whole body luciferase readings (**Figure 7E)**. The metastasis to liver is especially predominant, which dwarfed signals from the rest of the body (data not shown). As a result, I compared the readings from the mouse limb area only, which are presumably bone metastasis. To my surprise, I found that Nur77 WT mice had higher metastasis signals than Nur77 -/- mice **(Figure 7F),** which countered my original hypothesis. This could be due to the small sample size, big variation in luciferase reading, and the fact that B16 melanoma cells do not exclusively metastasize to bone, which makes experimental results hard to interpret. In addition, not every mouse in the experiment developed luciferase signal, despite the success of our intra cardiac injection procedure. This could be due to the mix background of our Nur77 KO mice, which makes it less compatible with B16 melanoma cells.

On the other hand, given that our Nur77 mice are whole body KO mice, it is possible that Nur77's systemic immune/inflammtory phenotype (McMorrow and Murphy, 2011)(or other systemic effects) against cancer overshadowed osteoclast's effect on bone metastasis. Interestingly, despite established publication that links Nur77 and cancer development (To et al., 2012), there is limited information on how Nur77 regulate cancer metastasis both within the cancer cells, and by modulating the host's immune function, etc. This could be an exciting area for further investigation.

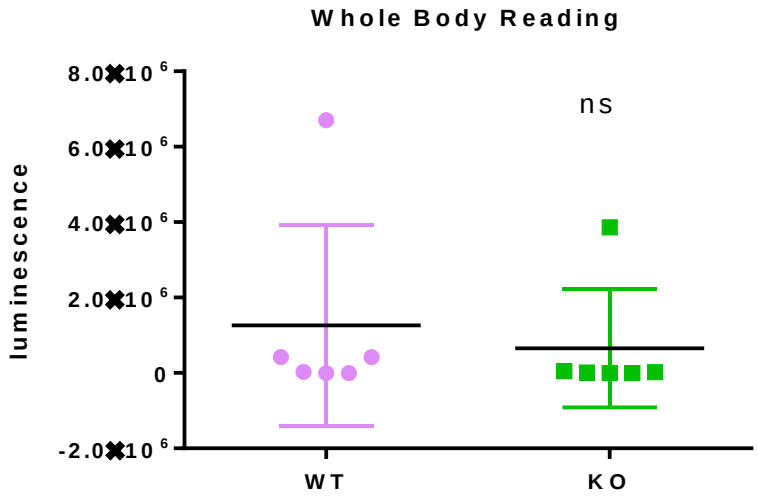

(Figure 7E) Luciferase imaging of B16 melanoma whole body metastasis in mice.

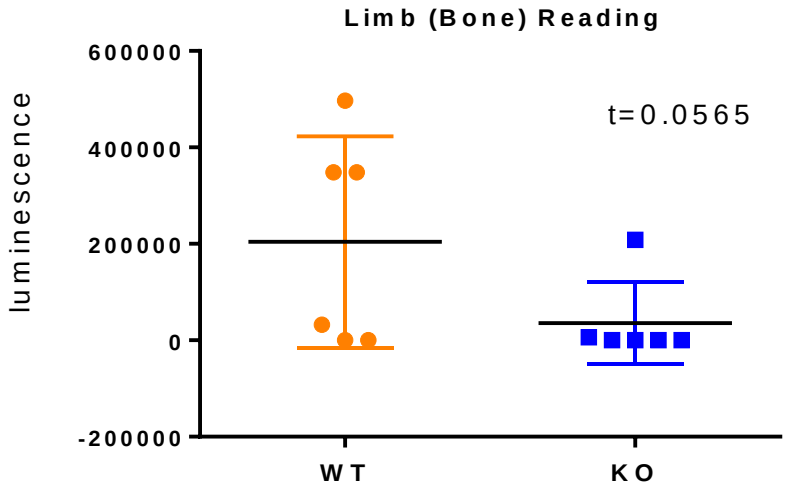

(Figure 7F) Luciferase imaging of B16 melanoma bone metastasis in mice.

Given all the caveats associated with the B16 melanoma mice model, I decided to breed Nur77 -/- mice to a nude background, so that they are immune compromised enough to receive bone-metastasis-prone MDA-MB-231 human breast cancer cell sub-line (MDA231-BoM-1833). To my surprise, when injected with 1833 cells, all of the nude Nur77 -/- mice died within 2-3 weeks, while almost all WT nude mice survived at least more than 7 weeks post injection **(Figure 7G).** The nude Nur77 -/- mice did not develop luciferase signal at 2 weeks post injection, which is unsurprising given luciferase signals usually start showing after 4 weeks. However, it does not explain why all of the nude Nur77 -/- mice died. Given Nur77's function in the immune system or other systems discussed before, it is also possible that nude Nur77 -/- experienced a stronger host versus graft rejection, compared with WT. While loss of Nur77 on a B6 background caused mild reduction of cancer metastasis, Nur77 loss on a nude background had probably caused even stronger anti-cancer immune response, and that mice on nude background are too weak to endure the inflammatory process. Further studies need to be done to dissect Nur77's role in modulating host's response to cancer metastasis, by selectively deleting Nur77 in different tissues.

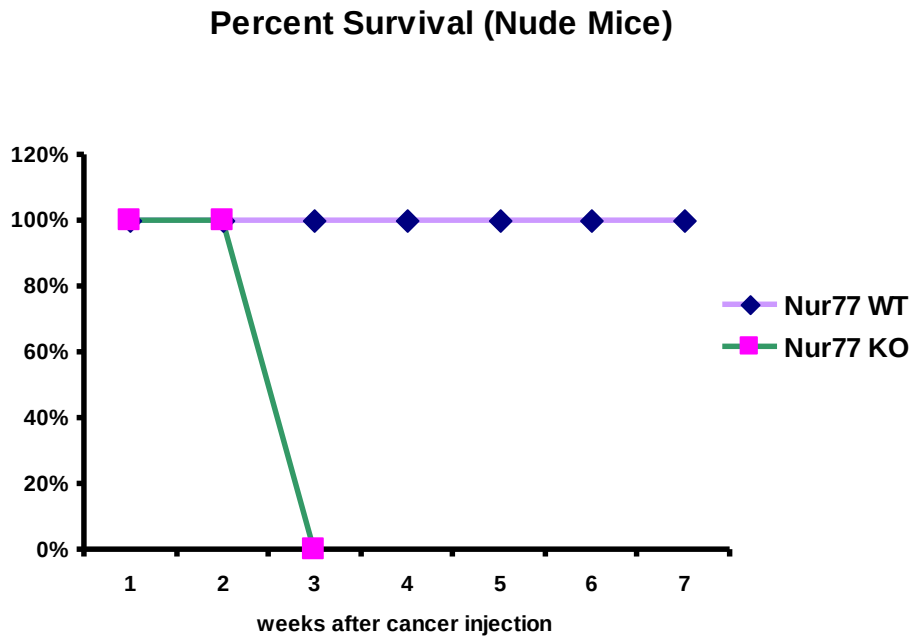

(Figure 7G) Survival rate of nude mice post intra-cardiac injection of cancer cells.

All together, these findings suggest that Nur77 regulation of osteoclastogenesis and bone homeostasis may be evolutionarily conserved and is relevant in several human skeletal diseases, such as osteoarthritis, cancer bone metastasis. It will be interesting to explore Nur77's potential role to serve as a novel therapeutic target in the treatment of human skeletal diseases.

Therapeutic Strategies to utilize the Nur77-Cbl-b-NFATc1 pathway

Given Nur77's important role in osteoclast development, bone resorption, and potentially osteoporosis, osteoarthritis and fracture healing, my next goals is to test strategies to activate Nur77 activity. Nur77 is an orphan receptor whose nature ligand has not been defined yet. However, there are several studies that suggested that cytosporone B could be a Nur77 activator (Lee et al., 2011). To test the specificity and efficacy of this compound in osteoclast differentiation, I treated both WT and Nur77 -/- bone marrow derived osteoclasts with varying amount of cytosporone B. My results showed that indeed, cytosporone B treatment lowered osteoclast differentiation, as shown by TRAP marker **(Figure 8A)**. However, Nur77 -/- osteoclast did not abolish cytosporone B's suppression of osteoclast diffentiation, raising questions on how specific this compound is to Nur77. To further study whether this cytosporone B's suppression effect is due to activation of Nur77 activity, I co-transfected Nur77 and NurRE-luciferase reporter into HEK293 cells, and treated the cultures with varying concentration cytosporone B. To my disappointment, cytosprone B did not play a role in NurRE activation **(Figure 8 B).** This could be caused by non-optimal treatment concentration and duration. But in concert with the non-specificity of the drug and the finding that NR4A1 family of proteins lack functional ligand binding domains, I concluded that seeking a ligand to activate Nur77 is probably not the best direction to go.

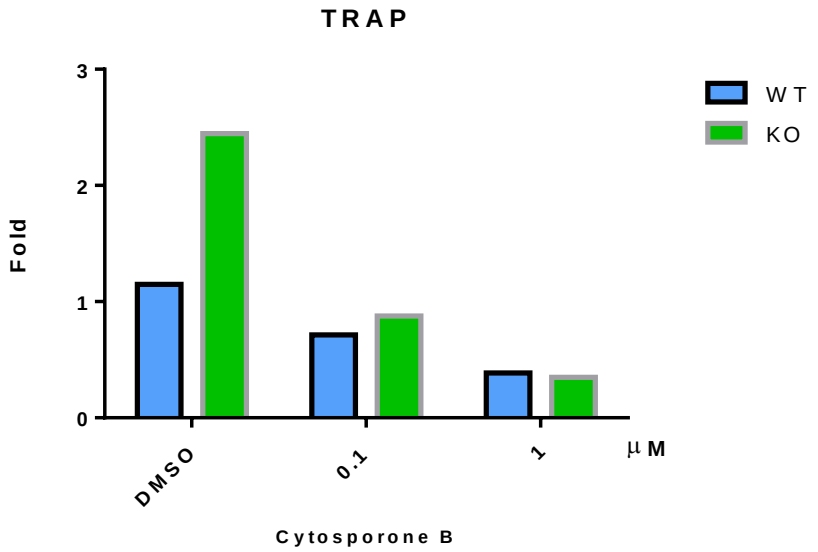

(Figure 8A) Osteoclast differentiation culture treated with vehicle (DMSO) and cytosporone B.

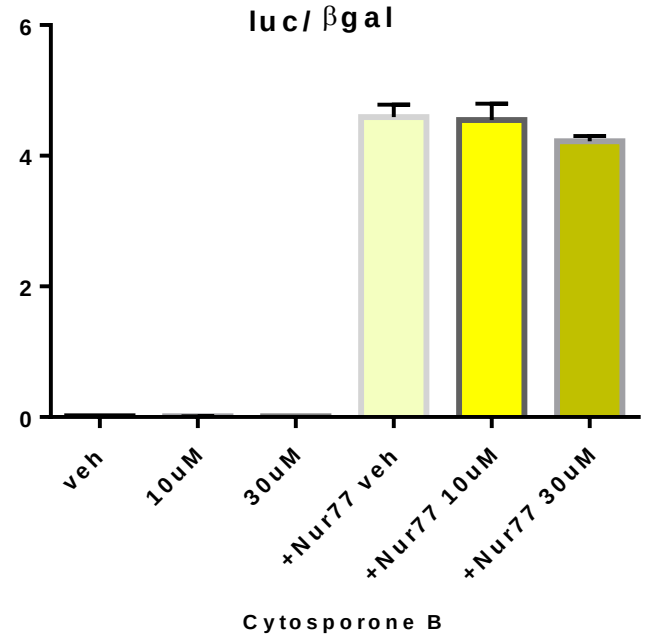

(Figure 8B) Transcription output of NurRE luc with different cytosporone B treatment

Another way to increase Nur77 activity is to increase its transcription. Micro RNAs (miRs) have been recently shown to regulate mRNA transcription, and has the potential to be used therapeutically (Hayes et al., 2014). However, in order to up-regulate Nur77 activity, I need to first find micro-RNAs that regulate Nur77 transcription, and then design anti-microRNAs to deplete microRNAs and release Nur77 from suppression.

Using bioinformatics, I identified four MiRs that could regulate Nur77 level. Two of them, miR-let7-5p and miR-124-5p had detectable levels in osteoclast. In addition, their levels go down during osteoclast differentiation **(Figure 8C and 8D),** exactly opposite Nur77 expression time course **(Figure 1B).** This suggests that they could be potential negative regulator of Nur77. miR-124 has been previously shown to regulate osteoclast differentiation, and synthetic inhibitor that binds specifically to miR-124 enhanced osteoclast differentiation (Lee et al., 2013). This is in agreement with out hypothesis that we could potentially using anti-miR-124 to activate Nur77 and inhibit bone resorption. Let-7 has not been implicated in osteoclast development yet.

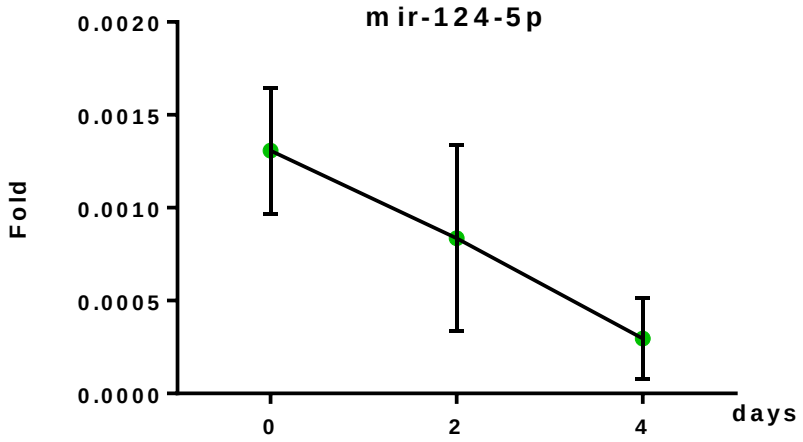

(Figure 8C) mir-124-5p expression during osteoclast differentiation

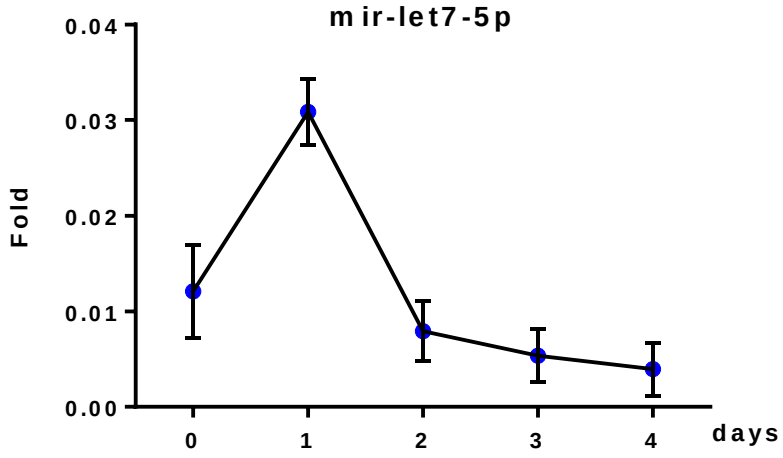

(Figure 8D) mir-let-7-5p expression during osteoclast differentiation

To study whether miR-124 or let-7 are effective at down regulating Nur77levels, I over-expressed either pre-miR-124 and pre-mir-let7 in osteoclast culture. My results showed that both miRs are effective at reduce Nur77 mRNA, with miR-124 being more effective. **(Figure 8E)** I next assessed whether this decrease in Nur77 mRNA is sufficient to lower Cbl-b level. qPCR data showed that both miRs can reduce Cbl-b level, although understandably to a lesser extent than Nur77 **(Figure 8F).** Interestingly NFATc1 mRNA is unchanged **(Figure 8G),** confirming our earlier hypothesis that Nur77 does not regulate NFATc1 at the transcriptional level. Finally, miR-124, but not miR-let-7, seem to be somewhat effective at up-regulating osteoclast marker TRAP through suppression of Nur77, although the effect is modest. **(Figure 8H)**

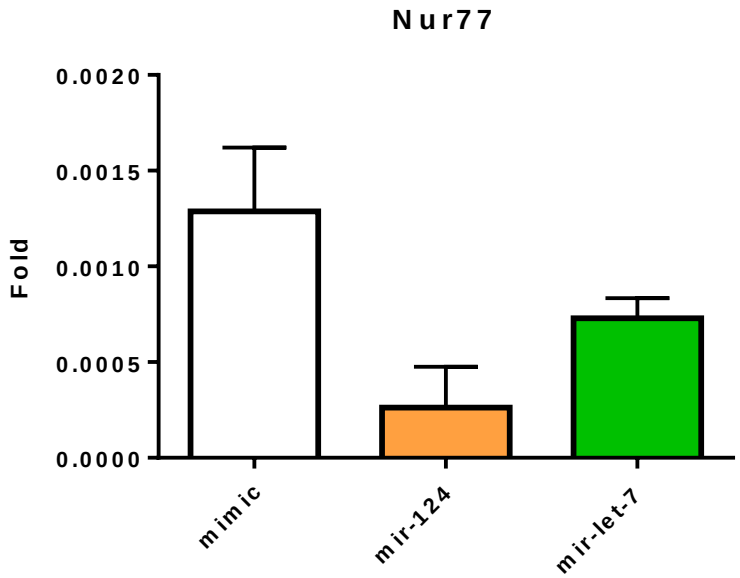

(Figure 8E) Nur77 level in osteoclast with treated with miRs

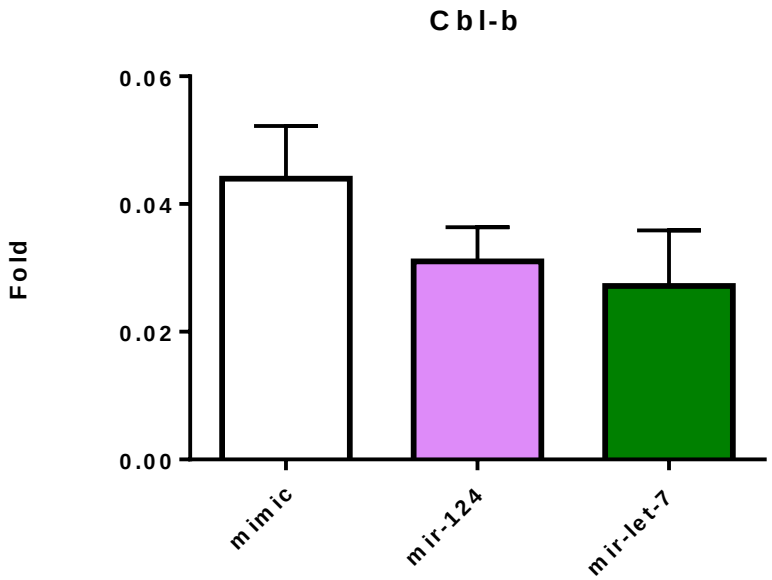

(Figure 8F) Cbl-b expression level in osteoclast treated with MiRs

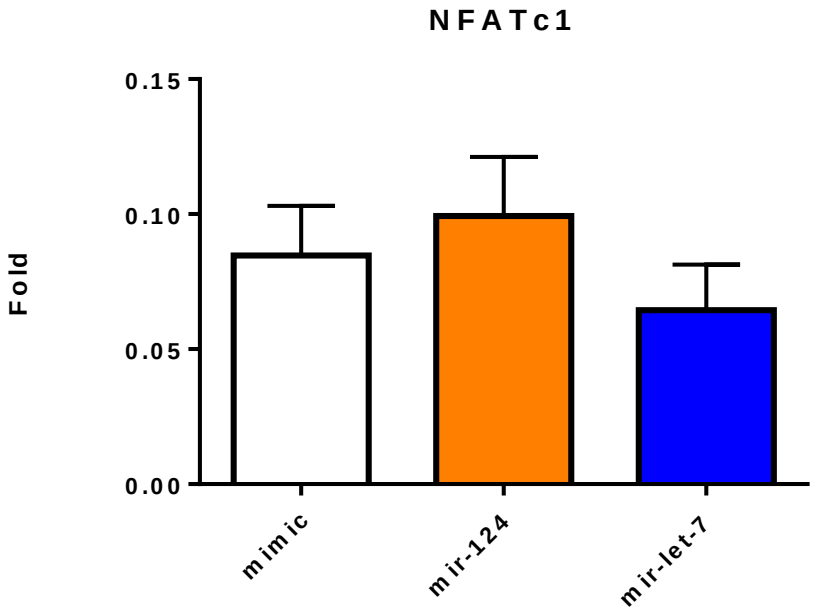

(Figure 8G) NFATc1 expression in osteoclast treated with MiRs

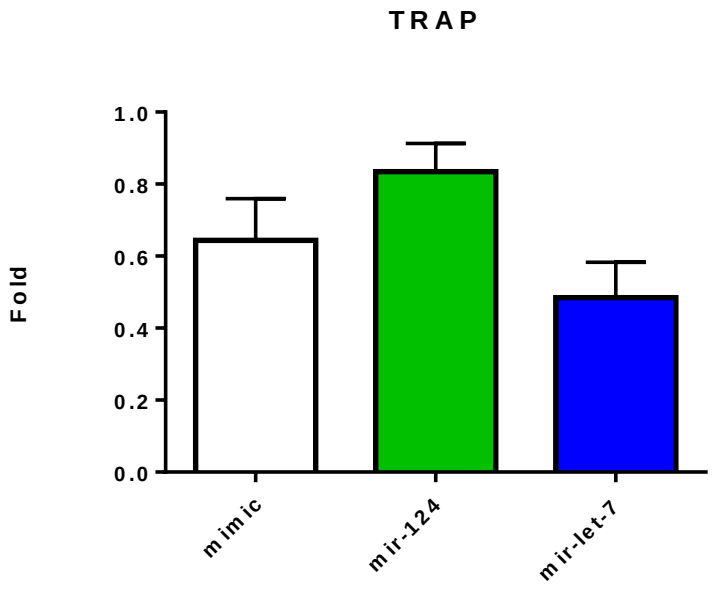

(Figure 8H) TRAP expression in osteoclast treated with MiRs

To therapeutically utilize the Nur77 pathway, I designed anti-miRs to deplete mir-124 and let-7. qPCR result showed that anti-miR-124, but not anti-let7 is effective at up-regulating Nur77 level. **(Figure 8I)** Unfortunately, anti-miR-124 was not able to significantly up-regulate Cbl-b level **(Figure 8J)**, or suppress osteoclast differentiation, as shown by TRAP expression **(Figure 8K)**. This could be due to several reasons. First, a two fold up-regulation of Nur77 **(Figure 8I)** is simply not large enough to cause significant change in Cbl-b and osteoclast differentiation. During osteoclast differentiation, Nur77 is up-regulated hundred of folds **(Figure 1B)** in order to induce sufficient Cbl-b change. Secondly, miR-124 or let-7's suppression of Nur77 might not be the key regulator of Nur77 level, so the release of their

suppression did not sufficiently induce Nur77 level. Finally, the anti-miR I used to treat osteoclast culture might be unstable in cells, or unable to bind to miRs in sufficient quantity, thus leaving residual miRs that could inhibit Nur77. This is especially true since the Lee et al. already showed that anti-miR-124 is effective at inhibiting osteoclast differentiation (Lee et al., 2013). Further optimizing treatment time, transfection efficiency and anti-MiR structure might improve the outcome.

Despite the above experimental outcome, using miR and anti-MiR offers a potential promising strategy to target key pathways in osteoclast differentiation to treat osteoclast related diseases.

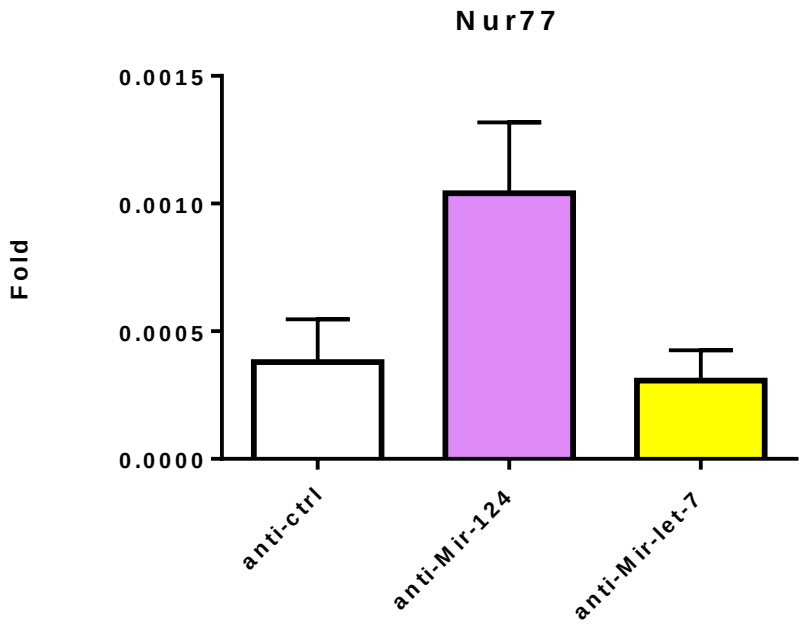

(Figure 8I) Nur77 expression in osteoclast, treated with anti-miRs

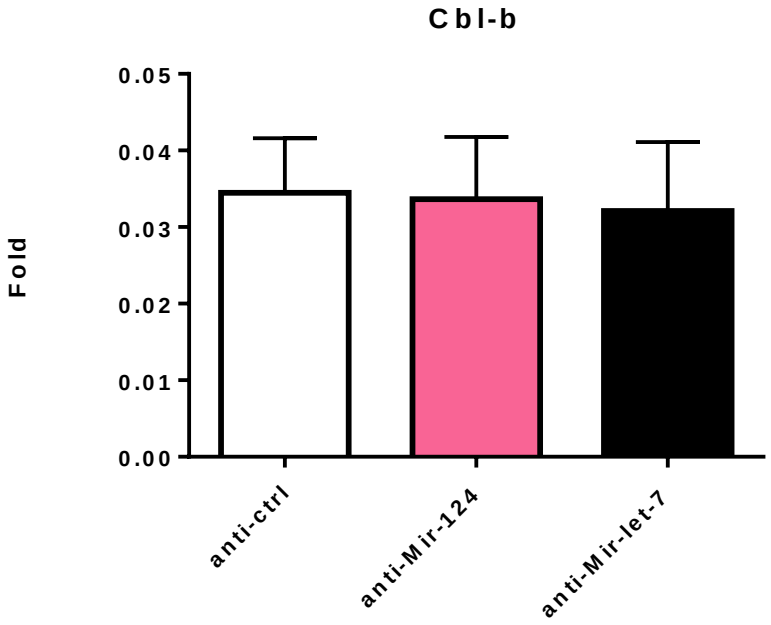

(Figure 8J) Cbl-b expression in osteoclast, treated with anti-miRs

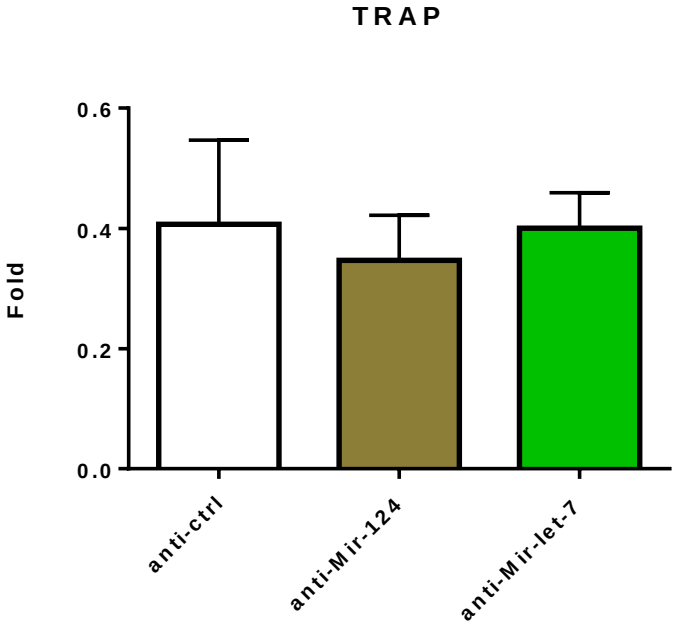

(Figure 8K) TRAP expression in osteoclast, treated with anti-miRs

Nur77 loss in fostering parents alters pup's bone metabolism

Bone development is regulated by both genetic and epigenetic factors. In my research of how Nur77 regulate bone metabolism, I unexpectedly found that Nur77 -/- pups born from Nur77 +/- parents have much higher CTX-1 values than Nur77 -/- pups born from Nur77 -/- Nor1 +/- parents **(Figure 9A)**. Given that the pups are of the same genotype and background, I hypothesized that this difference CTX-1 phenotype is due to the parental genotype. Since Nur77 +/- and Nor1 +/- mice tend to have similar phenotypes as WT mice, it is reasonable to consider that the difference is cause by WT vs Nur77 -/- parents.

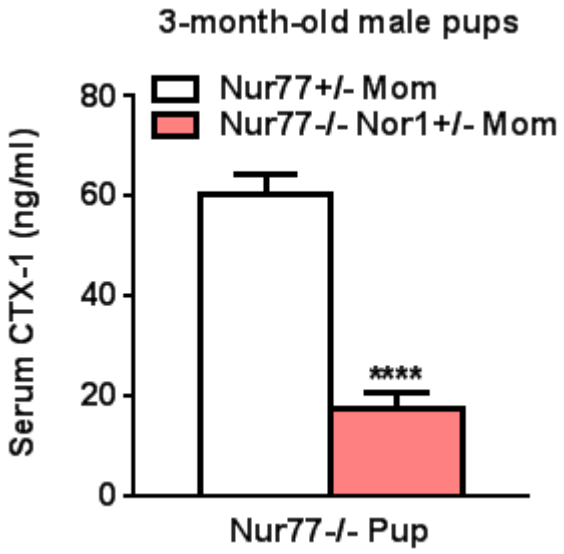

(Figure 9A) Serum CTX-1 level of Nur77 -/- pups born to either Nur77 +/- parents or Nur77 -/- Nor1 +/- parents.

To distinguish the pre-natal parental effect from post-natal parental influence on bone, I designed a cross foster experiment. WT pups born from WT parents are nursed by Nur77 -/- foster parents right after birth, and Nur77 -/- pups born to Nur77 -/- parents are nursed by WT foster parents. I tested the serum CTX-1 and P1NP levels in both WT and KO male pups at 2 month old. To my surprise, post-natal fostering alone seems to confer the parental effect on pup's bone. Both WT and Nur77 -/- pups fostered by Nur77 -/- parents have significantly lower CTX-1 value, or bone resorption, than pups fostered by KO parents **(Figure 9B)**. Even more interestingly, both WT and Nur77 -/- pups fostered by Nur77 -/- parents also have higher value of P1NP level (Figure 9C), or bone formation. These data showed that fostering parents with certain genetic traits can have a significant and protective effects on pups bone, and this effect lasts at least 2 months, and probably longer.

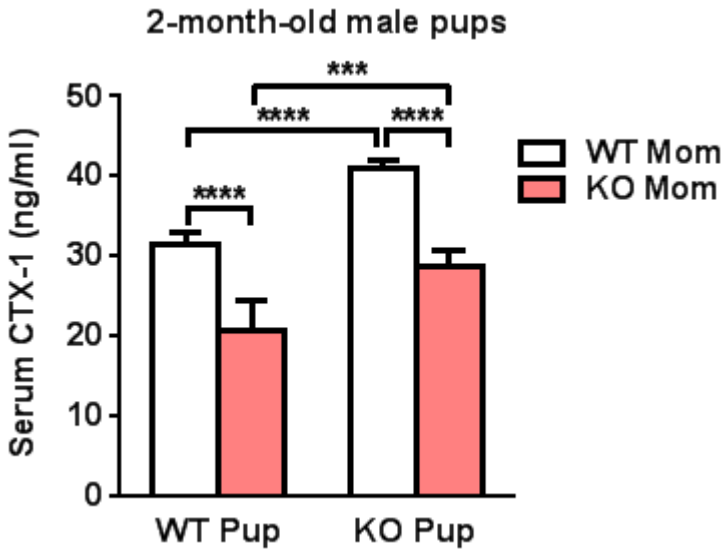

(Figure 9B) Serum CTX-1 value of WT and KO pups fostered by WT or KO parents

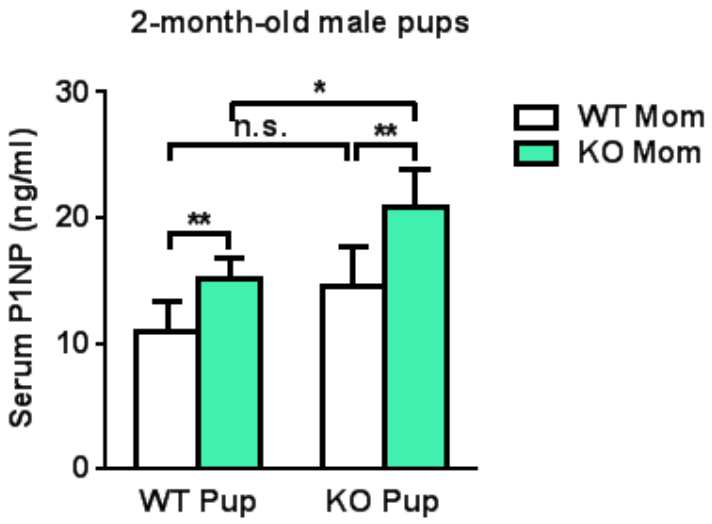

(Figure 9C) Serum P1NP value of WT and KO pups fostered by WT or KO parents

Given that fostered pups were raised under both paternal and maternal influence, I designed the next set of experiments to distinguish if the post natal parental effect on bone comes from the foster father, mother, or both. To achieve this goal, I compared Het pups born to WT mom, KO dad (mWT X dKO) or KO mom, WT dad (mKO X dWT) with Het mice born from Nur77 Het parents (which are close enough to WT parents). Surprisingly, having either a KO dad or a KO mom can significantly decrease pup's bone resorption and increase bone formation, and both KO mom and KO dad are equally good at influencing pup's phenotype. **(Figures 9E and 9F)**. As a result, pups' phenotype is most likely not caused by foster mother's milk content, but most likely from unique microbiota passed down from Nur77 KO parents.

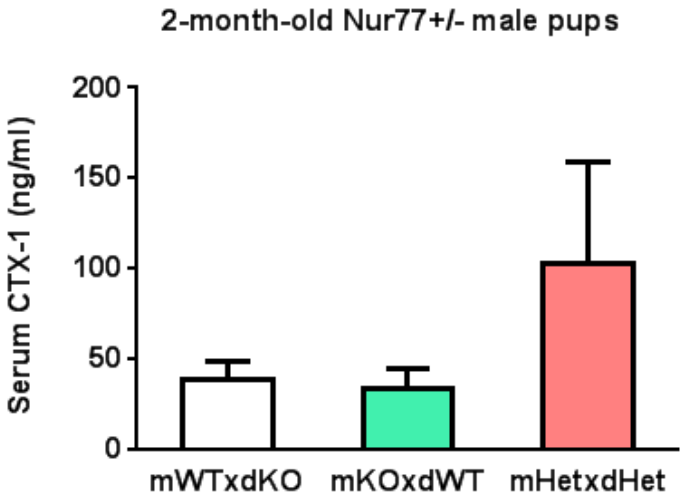

(Figure 9D) Serum CTX-1 level of Nur77 +/- pups born to parents with different genetic make up

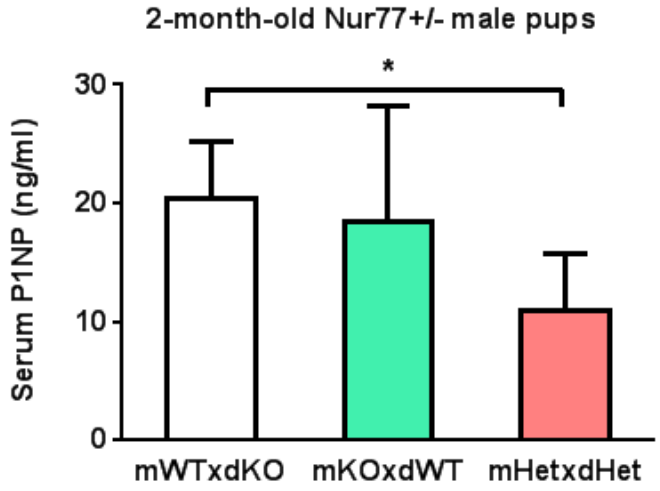

(Figure 9E) Serum P1NP level of Nur77 +/- pups born to parents with different genetic make up

Microbiota has been known to regulate a variety of physiological processes, but its role in bone is much less understood. It's been shown that compared with conventionally raised mice, germ-free mice has higher bone mass due to lower osteoclast number. (Sjogren et al., 2012) This is probably due to altered immune status in germ-free mice. It is very possible that Nur77 -/- parents possess a distinct set of microbiota due to their altered immune status, and are able to pass it down to their fostered new born pups, which are essentially germ free and are more likely to acquire the full set of microbiota from their fostering parents. These microbiota can then colonize the pups' body and have an protective effect in bone that last till adulthood.

To study specifically if the microbiota is responsible for causing the bone phenotype in pups, I designed two set of feces transfer experiments. In the first set, I sprayed WT pups born to WT parents (and raised by WT parents) with feces collected from Nur77-/- mice daily, in an attempt to initiate transferring of the Nur77 -/- microbiota. Conversely, I sprayed Nur77 -/- pups born to Nur77 -/- parents (and raised by Nur77 -/- parents) with WT feces daily. This set of experiments will not only tell me whether feces, or microbiota from mice feces, are responsible for causing the bone phenotype in pups, but also which microbiota set from WT or Nur77 -/- are more dominant and can out-compete the other. In addition, I also designed an experiment where I co-caged WT pups and their WT mother with a Nur77 -/- virgin female mouse, as a way to provide a sustainable source of microbiota.

I first measured the spleen weight of 1 month old female pups as a read out for their immune status change. To my surprise, WT pups receiving Nur77-/- feces and co-caged with a Nur77 -/- virgin female both had significantly higher spleen/body weight ratio, than WT control mice **(Figure 9F)**. There was no difference in spleen weight between either feces transfer or Nur77-/- co-caging, suggesting their mechanism of eliciting phenotype on pups are the same. On the other hand, Nur77 -/- pups receiving WT feces had comparable spleen weight to control pups **(Figure 9G).** These experiment suggests that the microbiota acquired from Nur77 -/- mice alone is able to change the immune status of pups, and that Nur77 -/- microbiota is the more dominant than WT. It will be very interesting to further study the immune phenotype such as serum cytokine levels, T cell, B cell, macrophage number and infiltrations etc, and test how long these immune changes last. Furthermore, it will be very exciting to see if feces transfer experiments can cause sufficient and lasting bone phenotype in pups. In addition, it will be interesting to see if the parental effect on pups' bone can be abolished by antibiotics treatment, which will further strength my hypothesis that microbiota is the cause of phenotype. Finally, it will be important to sequence the microbiota in both WT and Nur77 -/- mice to identify important microbes or microbial products that can be beneficial to bone development.

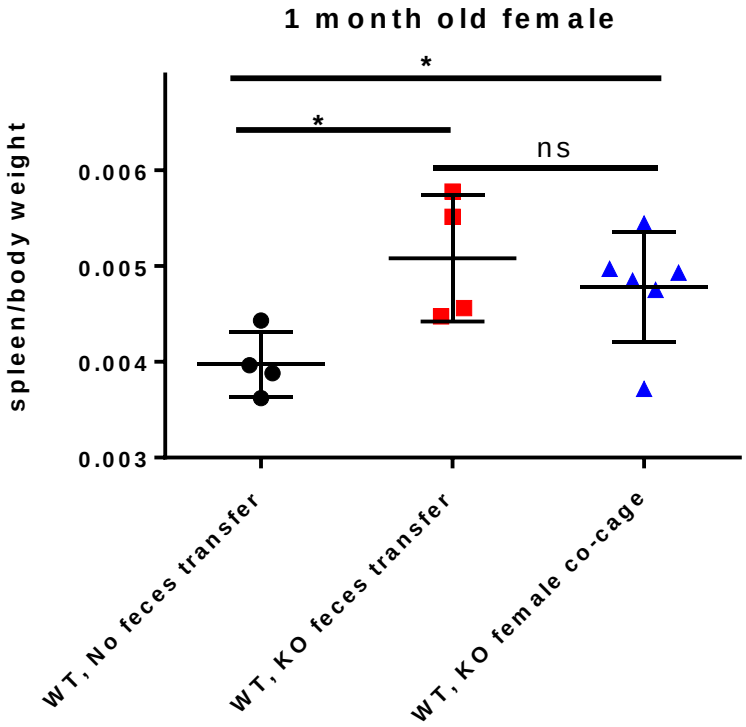

(Figure 9F) Spleen/body weight ratio of 1 month old WT female pups treated with either Nur77 -/- feces or with Nur77 -/- female co-caging.

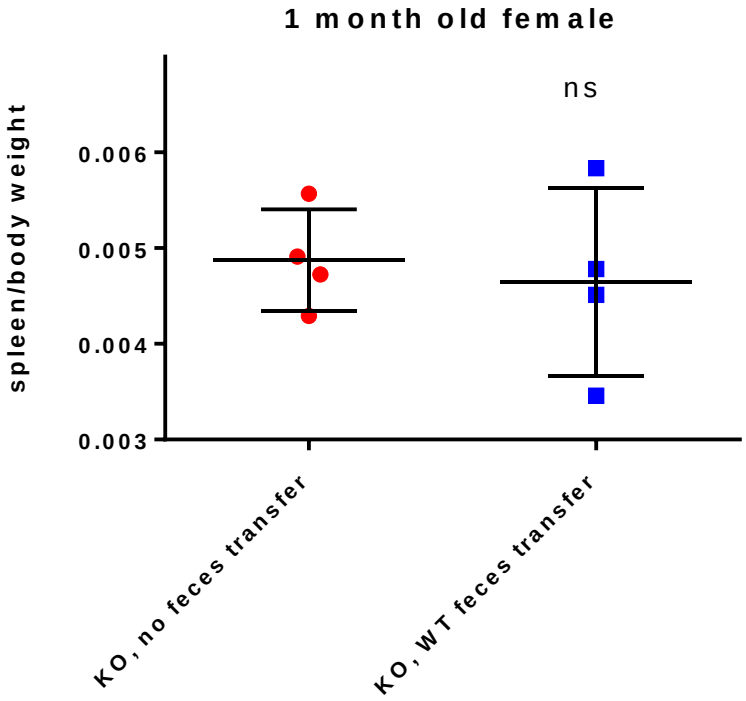

(Figure 9G) Spleen/body weight ratio of 1 month old female Nur77 -/- pups treated with WT feces.

Discussion

In this study, we have identified the nuclear receptor Nur77 as a critical negative regulator of osteoclastogenesis and bone resorption, revealing its novel bone protective role. Nur77 deletion causes elevated bone resorption and bone loss in mice; and low Nur77 levels correlates with degenerative skeletal disorders in human. Moreover, we have also unraveled a previously unrecognized mechanism for how Nur77 attenuates NFATc1 signaling at late stage of osteoclast differentiation. Nur77 can transcriptionally up-regulates Cbl-b E3 ligase to trigger NFATc1 protein degradation, so that NFATc1 signaling can be resolved in a timely fashion to prevent excessive osteoclastogenesis and bone resorption (**Figure 5E**).

In the process of studying the role of Nur77 in NFATc1 regulation and osteoclast differentiation, we inadvertently discovered that Nur77 is not only a regulator of NFATc1 but also a transcriptional target of NFATc1, thus revealing a negative feedback loop where NFATc1 induces its own degradation by up-regulating Nur77 and Cbl-b. This mechanism is crucial for proper cellular differentiation and function, since the resolution of signaling is just as important as its initiation and amplification. A breach in the NFATc1→Nur77→Cblb—•NFATc1 regulatory loop, exemplified by the Nur77-KO mice, will cause pathologically elevated NFATc1 levels during late stage of osteoclastogenesis and send osteoclasts into overdrive. To the best of our knowledge, we are the first group to propose an NFATc1 self-limiting regulatory mechanism. Therefore, NFATc1 exerts three functions to control

osteoclastogenesis. In addition to the previously recognized roles in its auto-amplification and activating osteoclast genes to initiate the differentiation, NFATc1 also plays a role in its auto-resolution to cease the differentiation (**Figure 5E**). Our findings will pave the road for future investigations to examine whether this NFATc1→Nur77→Cblb—•NFATc1 negative feedback loop may be widely applicable to NFATc1 regulation of other cellular processes such as T cell activation and cancer development.

Identification of novel osteoclast signaling pathways provides insights into potential new therapeutic options to treat bone degenerative diseases by inhibiting osteoclast activity. Current clinically approved osteoclast inhibitors, such as bisphosphonates and denosumab (anti-RANKL antibody), may cause severe side effects such as osteonecrosis of the jaw (ONJ) (Boquete-Castro et al., 2015; Khan et al., 2009). These side effects could stem from a variety of factors including target specificity. The whole body Nur77-KO mice, however, provides an example where despite the wide spread expression of a gene, it still can be targeted due to the differential sensitivity in different tissues. Although Nur77 has been implicated in numerous physiological functions *in vitro*, most of these functions did not hold true *in vivo* based on a general lack of phenotype in Nur77-KO mice (Chao et al., 2013; Lee et al., 1995). Until recently, Nur77-KO mice largely appear healthy and normal, and only exhibit clinical deficiencies under severe stress (Chao et al., 2009; Palumbo-Zerr et al., 2015) or with the deletion of an additional NR4A gene (Mullican et al., 2007). This may be partially due to functional redundancy among

NR4A family members so that the compensation by Nurr1 and Nor1 masks the effects of Nur77 loss. Interestingly, we found that Nur77 is the predominant NR4A member in the osteoclast lineage with little or no Nurr1 or Nor1 expression (**Figure 1B**), explaining the critical role of Nur77 in osteoclastogenesis so that the effects on bone is evident by Nur77 deletion alone. This creates an exciting opportunity for selective drug targeting and precision medicine with minimal side effects. Most recently, Tontonoz et al have uncovered a muscle protective role of Nur77 as mice deficient in Nur77 alone exhibit reduced muscle mass and myofiber size (Kanis, 1994). Therefore, Nur77 activation may represent a promising therapeutic strategy for musculoskeletal degenerative diseases with dual benefits on muscle and bone.

Given that Nur77 most likely will not respond to ligand stimulation, it will be interesting to turn to alternative strategies to activate Nur77, such as by using miRs and anti-miRs. Even though in my own studies, I have not been able to identify a anti-miR that can successfully activate Nur77, it is an interesting direction to pursue nonetheless.

In addition, the crucial regulation of NFATc1 protein degradation by Nur77 and Cbl-b suggests that it may be therapeutically beneficial to accelerate RANKL signaling resolution during osteoclastogenesis. Indeed, defects in the components of ubiquitin and proteasome system have been implicated in diseases including cancer and neurodegenerative disorders (Popovic et al., 2014). Bortezomib, a peptide inhibitor of proteasome, has been approved for clinical usage in pathological settings such as refractory multiple myeloma (Richardson et al., 2005). The discovery of

pathway-specific ubiquitin-proteasome activators, however, is somewhat lagging behind. Nonetheless, oleuropein, a small molecule proteasome activator, has been shown to delay replicative senescence of human embryonic fibroblast (Katsiki et al., 2007). In addition, oleuropein treatment has been shown to inhibit osteoclast formation and suppress the loss of trabecular bone in ovariectomized mice (Hagiwara et al., 2011), giving hope that small molecules that selectively activate the protein degradation pathway may be a promising future therapeutic strategy for skeletal and other diseases.

Finally, how microbiota and other epigenetic changes can regulate bone homeostasis has not been thoroughly studied and is an interesting direction to pursue. If we could identify particular microorganisms or microbial products that can decrease bone resorption or increase bone formation, or both, it will be very beneficial to patients who suffer from skeletal diseases.

Materials and methods

Mice

Nur77-/- mice (Lee et al., 1995) in a C57BL/6 and 129SvJ hybrid background was originally generated by Jeffrey Milbrandt at Washington University School of Medicine and kindly provided by Orla Conneely at Baylor College of Medicine. Cbl-b -/- mice are obtained from Amgen. Mice were fed with standard chow ad libitum and kept on a 12-h light, 12-h dark cycle. All experiments were conducted using littermates. Bone marrow transplantation was performed as described (Krzeszinski et al., 2014; Wan et al., 2007). Briefly, bone marrow cells from 2-month-old male donor (WT or Nur77-KO) were intravenously transplanted via retro orbital injection into 2-month-old male recipients (WT or Nur77-KO) that were irradiated at lethal dose (1000 roentgen); the mice were analyzed 3 month post transplantation. Sample size estimate was based on power analyses performed using SAS 9.3 TS X64_7PRO platform at the UTSW Biostatistics Core. With the observed group differences and the relatively small variation of the *in vivo* measurements, n=4 and n=3 will provide >90% and >80% power at type I error rate of 0.05 (two-sided test), respectively. All protocols for mouse experiments were approved by the Institutional Animal Care and Use Committee of UTSW.

Bone Analyses

μCT was performed using a Scanco μCT-35 instrument (Scanco Medical) as

described (Wei et al., 2010). Histomorphometry were performed as described (Wan et al., 2007; Wei et al., 2011). Serum CTX-1 bone resorption marker and P1NP bone formation marker were measured with RatLaps^{TM} EIA kit and Rat/Mouse PINP EIA kit (Immunodiagnostic Systems), respectively. To analyze osteocyte gene expression, mouse femur was cut off at both ends to allow marrow cells to be flushed out with media. It was then soaked in PBS and spun down to remove residual marrow cells, and snap frozen in liquid nitrogen, stored at -80°C until RNA extraction.

Bone Metastasis Analyses

Using a VisualSonics Vevo770 small-animal ultrasound device, luciferase-labelled cancer cells were injected into the left cardiac ventricle so that they could bypass the lung and efficiently migrate to the bone. Bone metastases were detected and quantified weekly after injection by BLI using a Caliper Xenogen Spectrum instrument at University of Texas Southwestern small animal imaging core facility. The luciferase-labelled bone-metastasis-prone MDA-MB-231 human breast cancer cell sub-line (MDA231-BoM-1833) was provided by J. Massagué and injected into 8 weeks old male nude mice at 1×10^5 cells per mouse in 100 μl PBS. The luciferase-labelled B16-F10 mouse melanoma cell line was provided by K. Weilbaecher and injected into 8-week-old male C57BL/6J mice at 5×10^4 cells per mouse in 100 μl PBS.

Ex Vivo Osteoclast and Osteoblast Differentiation

Osteoclasts were differentiated from bone marrow cells as described (Wan et al., 2007). Briefly, hematopoietic bone marrow cells were purified with a 40 μm cell strainer, cultured for 16 hours with 5 ng/ml MCSF (R&DSystems) in α-MEM containing 10% FBS. Floating cells were then collected and differentiated with 40 ng/ml of M-CSF in α-MEM containing 10% FBS for 3 days (day -3 to day 0), then with 40 ng/ml of MCSF and 100 ng/ml of RANKL (R&D Systems) for 3-9 days (day 0 to day 9). Mature osteoclasts were identified as multinucleated (>3 nuclei) $TRAP^+$ cells on day 9. Osteoclast differentiation was quantified by the RNA expression of osteoclast markers on day 3 using RT-QPCR analysis. Osteoblast differentiation from bone marrow cells was performed as previously described (Wei et al., 2012; Wei et al., 2014). Briefly, bone marrow cells were cultured for 4 days in MSC media (Mouse MesenCult® Proliferation Kit, StemCell Technologies), then differentiated into osteoblast with α-MEM containing 10% FBS, 5 mM β-glycerophosphate and 100 μg/ml ascorbic acid for 9 days.

Reagents

Antibodies for NFATc1, total-c-Jun and IκBα, as well as cyclosporine A were purchased from Santa Cruz Biotechnology. Phospho (ser73)-c-Jun antibody was from Cell Signaling. Anti-Histone H3 (tri methyl K4) antibody was from Abcam. Antibodies for Flag and β-actin were from Sigma. MG132 was from Fisher. Western blot and ChIP assays were performed as previously described (Krzeszinski et al.,

2014; Wan et al., 2007). NFATc1 expression plasmid was purchased from Open Biosystems. Human-Flag-Nur77 expression plasmid was kindly provided by Orla Conneely lab. Nur77-ΔDBD expression plasmid was constructed by deleting the amino acid residues 270-335 from the WT Nur77 expression plasmid. RNA was reverse transcribed into cDNA using an ABI High Capacity cDNA RT Kit, and analyzed using real-time quantitative PCR (SYBR Green) in triplicate. All RNA expression was normalized by the ribosomal gene L19. miR-124 and let-7 precursor and negative control, miR-124 and let7 inhibitor (anti-miR) and negative control were from Life Technologies. All miRNA and siRNA were transfected with Lipofectamine RNAiMAX (Life Technologies) into bone-marrow osteoclast progenitors.

Promoter Analyses

Cbl-b-promoter-luc-WT and Nur77-promoter-luc were constructed by cloning 1Kb and 0.8Kb segment upstream of transcription start site into pGL4 luciferase vector. Cbl-b-luc-Mut1 and Cbl-b-luc Mut2 were created by introducing mutations to three residues in each NurRE region of Cbl-b promoter, using the QuikChange II XL Site-Directed Mutagenesis Kit (Agilent Technologies). NFATc1 transcriptional activity was quantified using pNFAT-Luc reporter (Agilent Technologies). For transient transfection, a luciferase reporter was co-transfected into HEK293 cells with expression plasmids for β-gal and factors to be tested using FuGENE HD reagent (Roche). Vector alone or a GFP expression plasmid served as a negative control.

Luciferase activity was measured 48 hours later and normalized by β-gal activity. All transfection experiments were performed in triplicates and repeated for at least three times.

CRISPR Constructs and Clone Screening

Plasmids for gRNA cloning and hCas9 expression were from Addgene. Oligos for gRNA were designed to target upstream and downstream of the NurRE in the Cbl-b promoter, and cloned into gRNA vector according to the instruction form George Church Laboratory. Both vectors for gRNAs, and the expression plasmids for hCas9 and GFP marker were co-transfected into HEK293 cells. GFP^+ cells were sorted into 96-well plates at 1 cell/well 48 hours later. Each clone was expanded, genomic DNA was amplified by PCR and genotyped by sequencing. Two independent clones with NurRE deletion were compared to WT control.

Patient Data

Patient data for fracture healing and rheumatoid arthritis (Ungethuem et al., 2010) were retrieved from NIH GEO databases. Accession numbers are GSM7631 for fracture healing and GSM34398 for rheumatoid arthritis.

Statistical Analyses

All statistical analyses were performed with Student's t-Test and represented as mean ± standard deviation (Wei et al.) unless noted otherwise. The p values were

designated as: *, $p<0.05$; **, $p<0.01$; ***, $p<0.005$; ****, $p<0.001$; n.s. non-significant ($p>0.05$).

Acknowledgments

I thank Dr. Orla Conneely (Baylor College of Medicine) for *Nur77-/-* mice and Flag-Nur77 plasmid; UT Southwestern Biostatistics Core for their assistance in my studies; Drs. Paul Dechow and Jerry Feng (Baylor College of Dentistry) for assistance with μCT and histomorphometry. I am also grateful to Dr. Xunde Wang for teaching me cloning and other cell and molecular biology techniques. This work was in part supported by NIH (R01 DK089113, YW), CPRIT (RP130145, YW), DOD BCRP Idea Award (BC122877, YW), March of Dimes (#6-FY13-137, YW), The Welch Foundation (I-1751, YW) and UTSW Endowed Scholar Startup Fund (YW). I declare that I have no financial conflict of interest.

References

Office of the Surgeon General (US) (2001). NIH Consensus Development Panel on Osteoporosis Prevention, Diagnosis, and Therapy, March 7-29, 2000: highlights of the conference. Southern medical journal *94*, 569-573.

Asagiri, M., Sato, K., Usami, T., Ochi, S., Nishina, H., Yoshida, H., Morita, I., Wagner, E.F., Mak, T.W., Serfling, E., et al. (2005). Autoamplification of NFATc1 expression determines its essential role in bone homeostasis. The Journal of experimental medicine *202*, 1261-1269.

Azim, H., and Azim, H.A., Jr. (2013). Targeting RANKL in breast cancer: bone metastasis and beyond. Expert review of anticancer therapy *13*, 195-201.

Boquete-Castro, A., Gomez-Moreno, G., Calvo-Guirado, J.L., Aguilar-Salvatierra, A., and Delgado-Ruiz, R.A. (2015). Denosumab and osteonecrosis of the jaw. A systematic analysis of events reported in clinical trials. Clinical oral implants research.

Boyce, B.F., and Xing, L. (2007a). Biology of RANK, RANKL, and osteoprotegerin. Arthritis research & therapy *9 Suppl 1*, S1.

Boyce, B.F., and Xing, L. (2007b). The RANKL/RANK/OPG pathway. Current osteoporosis reports *5*, 98-104.

Bruzzaniti, A., and Baron, R. (2006). Molecular regulation of osteoclast activity. Reviews in endocrine & metabolic disorders *7*, 123-139.

Chao, L.C., Soto, E., Hong, C., Ito, A., Pei, L., Chawla, A., Conneely, O.M.,

Tangirala, R.K., Evans, R.M., and Tontonoz, P. (2013). Bone marrow NR4A expression is not a dominant factor in the development of atherosclerosis or macrophage polarization in mice. Journal of lipid research *54*, 806-815.

Chao, L.C., Wroblewski, K., Zhang, Z., Pei, L., Vergnes, L., Ilkayeva, O.R., Ding, S.Y., Reue, K., Watt, M.J., Newgard, C.B., et al. (2009). Insulin resistance and altered systemic glucose metabolism in mice lacking Nur77. Diabetes *58*, 2788-2796.

Chiou, S.H., Shahi, P., Wagner, R.T., Hu, H., Lapteva, N., Seethammagari, M., Sun, S.C., Levitt, J.M., and Spencer, D.M. (2011). The E3 ligase c-Cbl regulates dendritic cell activation. EMBO reports *12*, 971-979.

Hagiwara, K., Goto, T., Araki, M., Miyazaki, H., and Hagiwara, H. (2011). Olive polyphenol hydroxytyrosol prevents bone loss. European journal of pharmacology *662*, 78-84.

Hayes, J., Peruzzi, P.P., and Lawler, S. (2014). MicroRNAs in cancer: biomarkers, functions and therapy. Trends in molecular medicine *20*, 460-469.

Hirasaka, K., Kohno, S., Goto, J., Furochi, H., Mawatari, K., Harada, N., Hosaka, T., Nakaya, Y., Ishidoh, K., Obata, T., et al. (2007). Deficiency of Cbl-b gene enhances infiltration and activation of macrophages in adipose tissue and causes peripheral insulin resistance in mice. Diabetes *56*, 2511-2522.

Hirayama, T., Danks, L., Sabokbar, A., and Athanasou, N.A. (2002). Osteoclast formation and activity in the pathogenesis of osteoporosis in rheumatoid arthritis. Rheumatology *41*, 1232-1239.

Hsu, H.C., Zhou, T., and Mountz, J.D. (2004). Nur77 family of nuclear hormone

receptors. Current drug targets. Inflammation and allergy *3*, 413-423.

Hu, Y.W., Zhang, P., Yang, J.Y., Huang, J.L., Ma, X., Li, S.F., Zhao, J.Y., Hu, Y.R., Wang, Y.C., Gao, J.J., et al. (2014). Nur77 decreases atherosclerosis progression in apoE(-/-) mice fed a high-fat/high-cholesterol diet. PloS one *9*, e87313.

Kanis, J.A. (1994). Assessment of fracture risk and its application to screening for postmenopausal osteoporosis: synopsis of a WHO report. WHO Study Group. Osteoporosis international : a journal established as result of cooperation between the European Foundation for Osteoporosis and the National Osteoporosis Foundation of the USA *4*, 368-381.

Katsiki, M., Chondrogianni, N., Chinou, I., Rivett, A.J., and Gonos, E.S. (2007). The olive constituent oleuropein exhibits proteasome stimulatory properties in vitro and confers life span extension of human embryonic fibroblasts. Rejuvenation research *10*, 157-172.

Khan, A.A., Sandor, G.K., Dore, E., Morrison, A.D., Alsahli, M., Amin, F., Peters, E., Hanley, D.A., Chaudry, S.R., Lentle, B., et al. (2009). Bisphosphonate associated osteonecrosis of the jaw. The Journal of rheumatology *36*, 478-490.

Kim, J.H., Kim, K., Jin, H.M., Song, I., Youn, B.U., Lee, S.H., Choi, Y., and Kim, N. (2010). Negative feedback control of osteoclast formation through ubiquitin-mediated down-regulation of NFATc1. The Journal of biological chemistry *285*, 5224-5231.

Krzeszinski, J.Y., Wei, W., Huynh, H., Jin, Z., Wang, X., Chang, T.C., Xie, X.J., He, L., Mangala, L.S., Lopez-Berestein, G., et al. (2014). miR-34a blocks osteoporosis

and bone metastasis by inhibiting osteoclastogenesis and Tgif2. Nature *512*, 431-435.

Kuroda, Y., and Matsuo, K. (2012). Molecular mechanisms of triggering, amplifying and targeting RANK signaling in osteoclasts. World journal of orthopedics *3*, 167-174.

Lee, S.L., Wesselschmidt, R.L., Linette, G.P., Kanagawa, O., Russell, J.H., and Milbrandt, J. (1995). Unimpaired thymic and peripheral T cell death in mice lacking the nuclear receptor NGFI-B (Nur77). Science *269*, 532-535.

Lee, S.O., Li, X., Khan, S., and Safe, S. (2011). Targeting NR4A1 (TR3) in cancer cells and tumors. Expert opinion on therapeutic targets *15*, 195-206.

Lee, Y., Kim, H.J., Park, C.K., Kim, Y.G., Lee, H.J., Kim, J.Y., and Kim, H.H. (2013). MicroRNA-124 regulates osteoclast differentiation. Bone *56*, 383-389.

Lutz-Nicoladoni, C., Wolf, D., and Sopper, S. (2015). Modulation of Immune Cell Functions by the E3 Ligase Cbl-b. Frontiers in oncology *5*, 58.

Maxwell, M.A., and Muscat, G.E. (2006). The NR4A subgroup: immediate early response genes with pleiotropic physiological roles. Nuclear receptor signaling *4*, e002.

McMorrow, J.P., and Murphy, E.P. (2011). Inflammation: a role for NR4A orphan nuclear receptors? Biochemical Society transactions *39*, 688-693.

Mullican, S.E., Zhang, S., Konopleva, M., Ruvolo, V., Andreeff, M., Milbrandt, J., and Conneely, O.M. (2007). Abrogation of nuclear receptors Nr4a3 and Nr4a1 leads to development of acute myeloid leukemia. Nature medicine *13*, 730-735.

Nakajima, A., Sanjay, A., Chiusaroli, R., Adapala, N.S., Neff, L., Itzsteink, C.,

Horne, W.C., and Baron, R. (2009). Loss of Cbl-b increases osteoclast bone-resorbing activity and induces osteopenia. Journal of bone and mineral research : the official journal of the American Society for Bone and Mineral Research *24*, 1162-1172.

Nakashima, T., Hayashi, M., Fukunaga, T., Kurata, K., Oh-Hora, M., Feng, J.Q., Bonewald, L.F., Kodama, T., Wutz, A., Wagner, E.F., et al. (2011). Evidence for osteocyte regulation of bone homeostasis through RANKL expression. Nature medicine *17*, 1231-1234.

Nau, M.M., and Lipkowitz, S. (2003). Comparative genomic organization of the cbl genes. Gene *308*, 103-113.

Nguyen, N.D., Ahlborg, H.G., Center, J.R., Eisman, J.A., and Nguyen, T.V. (2007). Residual lifetime risk of fractures in women and men. Journal of bone and mineral research : the official journal of the American Society for Bone and Mineral Research *22*, 781-788.

Palumbo-Zerr, K., Zerr, P., Distler, A., Fliehr, J., Mancuso, R., Huang, J., Mielenz, D., Tomcik, M., Furnrohr, B.G., Scholtysek, C., et al. (2015). Orphan nuclear receptor NR4A1 regulates transforming growth factor-beta signaling and fibrosis. Nature medicine *21*, 150-158.

Paolino, M., Choidas, A., Wallner, S., Pranjic, B., Uribesalgo, I., Loeser, S., Jamieson, A.M., Langdon, W.Y., Ikeda, F., Fededa, J.P., et al. (2014). The E3 ligase Cbl-b and TAM receptors regulate cancer metastasis via natural killer cells. Nature *507*, 508-512.

Paolino, M., and Penninger, J.M. (2010). Cbl-b in T-cell activation. Seminars in immunopathology *32*, 137-148.

Paulsen, R.E., Weaver, C.A., Fahrner, T.J., and Milbrandt, J. (1992). Domains regulating transcriptional activity of the inducible orphan receptor NGFI-B. The Journal of biological chemistry *267*, 16491-16496.

Perlmann, T., and Jansson, L. (1995). A novel pathway for vitamin A signaling mediated by RXR heterodimerization with NGFI-B and NURR1. Genes & development *9*, 769-782.

Philips, A., Lesage, S., Gingras, R., Maira, M.H., Gauthier, Y., Hugo, P., and Drouin, J. (1997). Novel dimeric Nur77 signaling mechanism in endocrine and lymphoid cells. Molecular and cellular biology *17*, 5946-5951.

Popovic, D., Vucic, D., and Dikic, I. (2014). Ubiquitination in disease pathogenesis and treatment. Nature medicine *20*, 1242-1253.

Qiao, G., Lei, M., Li, Z., Sun, Y., Minto, A., Fu, Y.X., Ying, H., Quigg, R.J., and Zhang, J. (2007). Negative regulation of CD40-mediated B cell responses by E3 ubiquitin ligase Casitas-B-lineage lymphoma protein-B. Journal of immunology *179*, 4473-4479.

Richardson, P.G., Sonneveld, P., Schuster, M.W., Irwin, D., Stadtmauer, E.A., Facon, T., Harousseau, J.L., Ben-Yehuda, D., Lonial, S., Goldschmidt, H., et al. (2005). Bortezomib or high-dose dexamethasone for relapsed multiple myeloma. The New England journal of medicine *352*, 2487-2498.

Richardson, P.G., Xie, W., Jagannath, S., Jakubowiak, A., Lonial, S., Raje, N.S.,

Alsina, M., Ghobrial, I.M., Schlossman, R.L., Munshi, N.C., et al. (2014). A phase 2 trial of lenalidomide, bortezomib, and dexamethasone in patients with relapsed and relapsed/refractory myeloma. Blood *123*, 1461-1469.

Roodman, G.D. (2004). Mechanisms of bone metastasis. The New England journal of medicine *350*, 1655-1664.

Schell, H., Lienau, J., Epari, D.R., Seebeck, P., Exner, C., Muchow, S., Bragulla, H., Haas, N.P., and Duda, G.N. (2006). Osteoclastic activity begins early and increases over the course of bone healing. Bone *38*, 547-554.

Schett, G., Hayer, S., Zwerina, J., Redlich, K., and Smolen, J.S. (2005). Mechanisms of Disease: the link between RANKL and arthritic bone disease. Nature clinical practice. Rheumatology *1*, 47-54.

Sjogren, K., Engdahl, C., Henning, P., Lerner, U.H., Tremaroli, V., Lagerquist, M.K., Backhed, F., and Ohlsson, C. (2012). The gut microbiota regulates bone mass in mice. Journal of bone and mineral research : the official journal of the American Society for Bone and Mineral Research *27*, 1357-1367.

Takayanagi, H., Kim, S., Koga, T., Nishina, H., Isshiki, M., Yoshida, H., Saiura, A., Isobe, M., Yokochi, T., Inoue, J., et al. (2002). Induction and activation of the transcription factor NFATc1 (NFAT2) integrate RANKL signaling in terminal differentiation of osteoclasts. Developmental cell *3*, 889-901.

Tanaka, S. (2013). Regulation of bone destruction in rheumatoid arthritis through RANKL-RANK pathways. World journal of orthopedics *4*, 1-6.

To, S.K., Zeng, J.Z., and Wong, A.S. (2012). Nur77: a potential therapeutic target in

cancer. Expert opinion on therapeutic targets *16*, 573-585.

Ungethuem, U., Haeupl, T., Witt, H., Koczan, D., Krenn, V., Huber, H., von Helversen, T.M., Drungowski, M., Seyfert, C., Zacher, J., et al. (2010). Molecular signatures and new candidates to target the pathogenesis of rheumatoid arthritis. Physiological genomics *42A*, 267-282.

Wan, Y., Chong, L.W., and Evans, R.M. (2007). PPAR-gamma regulates osteoclastogenesis in mice. Nat Med *13*, 1496-1503.

Wansa, K.D., Harris, J.M., and Muscat, G.E. (2002). The activation function-1 domain of Nur77/NR4A1 mediates trans-activation, cell specificity, and coactivator recruitment. The Journal of biological chemistry *277*, 33001-33011.

Wei, W., Dutchak, P.A., Wang, X., Ding, X., Bookout, A.L., Goetz, R., Mohammadi, M., Gerard, R.D., Dechow, P.C., Mangelsdorf, D.J., et al. (2012). Fibroblast growth factor 21 promotes bone loss by potentiating the effects of peroxisome proliferator-activated receptor gamma. Proc Natl Acad Sci U S A *109*, 3143-3148.

Wei, W., Motoike, T., Krzeszinski, J.Y., Jin, Z., Xie, X.J., Dechow, P.C., Yanagisawa, M., and Wan, Y. (2014). Orexin Regulates Bone Remodeling via a Dominant Positive Central Action and a Subordinate Negative Peripheral Action. Cell Metab.

Wei, W., Wang, X., Yang, M., Smith, L.C., Dechow, P.C., Sonoda, J., Evans, R.M., and Wan, Y. (2010). PGC1beta mediates PPARgamma activation of osteoclastogenesis and rosiglitazone-induced bone loss. Cell Metab *11*, 503-516.

Wei, W., Zeve, D., Suh, J.M., Wang, X., Du, Y., Zerwekh, J.E., Dechow, P.C., Graff,

J.M., and Wan, Y. (2011). Biphasic and dosage-dependent regulation of osteoclastogenesis by beta-catenin. Mol Cell Biol *31*, 4706-4719.

Weinstein, R.S., Roberson, P.K., and Manolagas, S.C. (2009). Giant osteoclast formation and long-term oral bisphosphonate therapy. The New England journal of medicine *360*, 53-62.

Whitaker, M., Guo, J., Kehoe, T., and Benson, G. (2012). Bisphosphonates for osteoporosis--where do we go from here? The New England journal of medicine *366*, 2048-2051.

Zupan, J., Jeras, M., and Marc, J. (2013). Osteoimmunology and the influence of pro-inflammatory cytokines on osteoclasts. Biochemia medica *23*, 43-63.